

1 **The Imposition of Value on Odor: Transient and Persistent Representations of**  
2 **Odor Value in Prefrontal Cortex**

3 Peter Y. Wang<sup>1,4</sup>, Cristian Boboila<sup>1,4</sup>, Philip Shamash<sup>1,3</sup>, Zheng Wu<sup>1</sup>, Nicole P Stein<sup>1</sup>,  
4 L.F. Abbott<sup>1</sup>, Richard Axel<sup>1,2,5\*</sup>

5

6 <sup>1</sup> The Mortimer B. Zuckerman Mind Brain Behavior Institute, Department of  
7 Neuroscience, Columbia University, New York, NY 10027, USA

8 <sup>2</sup> Howard Hughes Medical Institute, Columbia University

9 <sup>3</sup> Present address: Sainsbury Wellcome Center for Neural Circuits and Behavior,  
10 University College London, London W1T 4AY, UK

11 <sup>4</sup> Co-first author

12 <sup>5</sup> Lead Contact

13

14 \* Correspondence: ra27@columbia.edu (R.A.)

15 **SUMMARY**

16           The representation of odor in olfactory cortex (piriform) is distributive and  
17 unstructured and can only be afforded behavioral significance upon learning. We  
18 performed 2-photon imaging to examine the representation of odors in piriform and in  
19 two downstream stations, the orbitofrontal cortex (OFC) and medial prefrontal cortex  
20 (mPFC), as mice learned olfactory associations. In piriform we observed minor changes  
21 in neural activity unrelated to learning. In OFC, 30% of the neurons acquired robust  
22 responses to conditioned stimuli (CS+) after learning, and these responses were gated  
23 by context and internal state. The representation in OFC, however, diminished after  
24 learning and persistent representations of CS+ and CS- odors emerged in mPFC.  
25 Optogenetic silencing indicates that these two brain structures function sequentially to  
26 consolidate the learning of appetitive associations. These data demonstrate the  
27 transformation of a representation of odor identity in piriform into transient and  
28 persistent representations of value in the prefrontal cortex.

## 29 INTRODUCTION

30 Most organisms have evolved a mechanism to recognize olfactory information in  
31 the environment and transmit this information to the brain where it must be processed to  
32 create an internal representation of the external world. This representation must  
33 translate stimulus features into appropriate behavioral responses. The olfactory sensory  
34 system does not merely represent the external world. Rather it interprets features of the  
35 world and combines them in higher cortical centers to construct representations that  
36 encode both the identity and value of different odors. Only two synapses intervene  
37 between the nose and the olfactory cortex, the piriform. Piriform cortex projects directly  
38 to higher order brain structures such as the orbitofrontal cortex (OFC) and medial  
39 prefrontal cortex (mPFC) (Chen et al., 2014; Diodato et al., 2016; Price, 1985). This  
40 shallow and well-characterized sensory pathway affords us the ability to identify the  
41 circuits that transform the identity of a sensory stimulus into representations of value  
42 that guide behavior.

43

44 Olfactory perception is initiated by the recognition of odorants by a large  
45 repertoire of receptors in the sensory epithelium (Buck and Axel, 1991; Godfrey et al.,  
46 2004; Zhang and Firestein, 2002). Individual sensory neurons in mice express only one  
47 of 1100 different receptor genes, and neurons that express the same receptor project  
48 with precision to two spatially invariant glomeruli in the olfactory bulb (Mombaerts et al.,  
49 1996; Ressler et al., 1993, 1994; Vassar et al., 1994). Thus, a transformation in the  
50 representation of olfactory information is apparent in the bulb where a dispersed  
51 population of active neurons in the sense organ is consolidated into a discrete spatial

52 map of glomerular activity (Bozza et al., 2004). Each odorant activates a unique  
53 ensemble of glomeruli and the recognition of an odor requires integration of information  
54 from multiple glomeruli in higher olfactory centers.

55

56 The projection neurons of the olfactory bulb, the mitral and tufted cells, extend an  
57 apical dendrite into a single glomerulus and send axons to several telencephalic areas  
58 including significant input to piriform cortex (Price and Powell, 1970). Anatomic tracing  
59 reveals that axonal projections from individual glomeruli discard the spatial patterning of  
60 the bulb and diffusely innervate the piriform (Ghosh et al., 2011; Sosulski et al., 2011).  
61 Electrophysiologic and optical recordings demonstrate that individual odorants activate  
62 subpopulations of neurons distributed across the piriform without apparent spatial  
63 preference (Illig and Haberly, 2003; Iurilli and Datta, 2017; Poo and Isaacson, 2009;  
64 Rennaker et al., 2007; Stettler and Axel, 2009; Sugai et al., 2005; Zhan and Luo, 2010).  
65 Moreover, exogenous activation of an arbitrarily chosen ensemble of piriform neurons  
66 can elicit behaviors of contrasting valence dependent on learning (Choi et al., 2011).  
67 These observations are consistent with a model in which individual piriform cells receive  
68 convergent input from a random collection of glomeruli (Davison and Ehlers, 2011;  
69 Miyamichi et al., 2011; Stettler and Axel, 2009). In this model odor representations in  
70 piriform can only be afforded behavioral significance upon learning.

71

72 The piriform cortex sends projections to numerous brain regions including the  
73 amygdala, hippocampus, and prefrontal cortex, and is anatomically poised to  
74 accommodate the transformation of sensory representations into representations of

75 value that can lead to appropriate behavioral output (Chen et al., 2014; Diodato et al.,  
76 2016; Johnson et al., 2000; Price, 1985; Schwabe et al., 2004). Neurons in orbitofrontal  
77 cortex (OFC) in both rodents and primates represent value but also encode other task  
78 variables including stimulus identity, motor action, confidence, internal state and task  
79 context (Feierstein et al., 2006; Gottfried et al., 2003; Kepecs et al., 2008; Lipton et al.,  
80 1999; Namboodiri et al., 2019; Padoa-Schioppa and Assad, 2006; Ramus and  
81 Eichenbaum, 2000; Schoenbaum and Eichenbaum, 1995; Schoenbaum et al., 1998,  
82 1999; Thorpe et al., 1983; Tremblay and Schultz, 1999). Lesion experiments implicate  
83 OFC in updating learned information but these studies failed to reveal a role for OFC in  
84 simple associative learning (Bissonette et al., 2008; Burke et al., 2008; Chudasama and  
85 Robbins, 2003; Gallagher et al., 1999; Izquierdo et al., 2004; Ostlund and Balleine,  
86 2007; Schoenbaum et al., 2002; Stalnaker et al., 2007). Medial prefrontal cortex  
87 (mPFC) has been implicated in simple associative learning and the remodeling of  
88 learned information (Birrell and Brown, 2000; Bissonette et al., 2008; Chudasama and  
89 Robbins, 2003; Ferenczi et al., 2016; Kim et al., 2017; Kitamura et al., 2017; Ostlund  
90 and Balleine, 2005; Otis et al., 2017). Recently, a neural representation of rewarded  
91 auditory stimuli was identified in both OFC and mPFC, and silencing of these brain  
92 structures elicited deficits in the acquisition and expression of learned behavior  
93 (Namboodiri et al., 2019; Otis et al., 2017).

94

95 We have performed two photon endoscopic imaging in piriform, OFC, and mPFC  
96 during appetitive associative conditioning to identify brain structures that exhibit  
97 changes in their neural representations upon olfactory learning (Barretto et al., 2009;

98 Denk et al., 1990; Jung et al., 2004). Optogenetic silencing was then used to discern  
99 possible roles for these representations in associative conditioning. Imaging of neural  
100 activity in the piriform revealed that odor responses were sparse, selective, and  
101 unchanged by learning. Imaging of neural activity in the orbitofrontal cortex (OFC)  
102 revealed that 30% of OFC neurons acquired robust responses to conditioned (CS+) but  
103 not to unconditioned (CS-) odors during training. Moreover, these responses were gated  
104 by context and internal state. This representation in OFC diminished after learning, and  
105 persistent and non-overlapping representations of CS+ and CS- odors emerged in  
106 mPFC. Optogenetic silencing revealed that the OFC and mPFC appear to function  
107 sequentially in the learning of appetitive associations. These data demonstrate the  
108 transformation of a representation of odor identity in piriform into a transient  
109 representation of positive value in the OFC and then a persistent representation of  
110 positive and negative value in the mPFC.

111

## 112 **RESULTS**

### 113 **Representation of Odor Identity in Piriform Cortex**

114 We examined odor representations in piriform cortex while mice learned an  
115 appetitive odor discrimination task. Head fixed mice were exposed to two (CS+) odors  
116 that predicted a water reward delivered after a short delay and to two unrewarded (CS-)  
117 odors (Figure 1A). In separate trials the mice received a water reward (US) without prior  
118 odor delivery. After three to four training sessions, nearly all mice displayed anticipatory  
119 licking in response to the CS+ odors in over 90% of the trials (17 of 19 mice) and licked  
120 in fewer than 15% of the CS- trials (18 of 19 mice) (Figure 1B, 1C). We imaged neural

121 activity by 2-photon microscopy during training in 6 mice expressing GCaMP6s in  
122 excitatory neurons in the piriform (Barretto et al., 2009; Chen et al., 2013; Denk et al.,  
123 1990; Jung et al., 2004; Madisen et al., 2015; Vong et al., 2011). We recorded the  
124 activity of 359 piriform neurons in six mice during one week of learning. Before learning,  
125 the four odors each activated an average of 16% of the piriform neurons (Figure 1F,  
126 S1B). Less than 4% of the neurons in piriform responded to water without prior odor  
127 exposure (Figure 1E, S1B). The neural responses after learning were largely  
128 unchanged (Figure 1D, 1F, S1A, S1B, S1F-H). The ensemble evoked by a given odor  
129 prior to training was significantly correlated with the ensemble evoked by the same odor  
130 after four days of task learning (Figure 1G). In a separate series of experiments,  
131 across-day correlations were similarly high after four days of passive odor exposure  
132 (Figure 1G). We also measured the correlation between the ensemble activities evoked  
133 by pairs of distinct odors. We found that the correlations between pairs of odor  
134 ensembles were low prior to learning and decreased even further after learning (Figure  
135 1H, 1I; before learning: 0.50, after learning: 0.32,  $p < 0.001$ , Wilcoxon signed-rank test.).  
136 These results suggest that odor representations are stable but become slightly more  
137 discriminable across multiple training days.

138

139 These conclusions are further supported by decoding analysis (Figure S1C). A  
140 linear decoder trained on population activity prior to learning distinguished the identities  
141 of the four odors using population activity after learning (day 4 of training) with greater  
142 than 75% accuracy (Figure 1J). The odor ensembles became slightly more separable  
143 as training proceeded (Figure 1J), but these changes were qualitatively similar for both

144 CS+ and CS- odor ensembles (Figure S1D, S1E), and also occurred upon passive odor  
145 exposure (Figure S1F-K). Thus, minor changes were observed in the representation of  
146 odors after training, but these changes were observed for both CS+ and CS- odors and  
147 were not dependent upon learning. These experiments suggest that changes in the  
148 representation of odor in the piriform do not reflect learning, and neural instantiations of  
149 learning must occur downstream.

150

### 151 **A Representation of Value in Orbitofrontal Cortex**

152 The piriform cortex sends axons to numerous brain regions, with an extensive  
153 projection to orbitofrontal cortex (Chen et al., 2014; Price, 1985). We therefore asked  
154 whether appetitive odor learning elicits changes in the representation of odors in OFC.  
155 We imaged the activity of 364 OFC neurons in 5 animals across multiple training days.  
156 Before learning, the four odors each activated an average of 12% of the neurons in  
157 OFC (Figure 2A, S2B). The responses were non-selective, inconsistent, and low in  
158 amplitude (Figure 2A, 2C, S2A). 16% of imaged neurons responded to water, the  
159 unconditioned stimulus (Figure S2B). In contrast to piriform cortex, we could not discern  
160 a representation of odor identity in OFC prior to learning (see below).

161

162 We observed a striking change in the neuronal response to CS+ odors as  
163 learning proceeded (Figure 2B, 2C). After learning, 30% of the OFC neurons acquired  
164 consistent, high amplitude responses to each of the two CS+ odors (Figure S2B). 75%  
165 of neurons responsive to one CS+ odor also responded to the second CS+ odor (Figure  
166 S2C). Moreover, the amplitude and duration of responses to the two CS+ odors in a



167 given neuron were similar (Figure S2D, S2E). 64% of the CS+ responsive neurons were  
168 not activated in water-only trials, demonstrating that the majority of these CS+  
169 responses did not result from the activation of a motor program (Figure 2B). After  
170 learning, CS- odors continued to elicit sparse, inconsistent, and low amplitude  
171 responses, similar to the responses observed prior to training (Figure 2B-D, S2B).  
172 These observations suggest projections from the CS+ representation in piriform to the  
173 OFC are reinforced during learning.

174

175         The mean excitatory response amplitude (which we call the response power)  
176 evoked by CS+ odors increased almost three-fold (286%) after learning, with only a  
177 minor (138%) change in response power to CS- odors (Figure 2D). Moreover, the  
178 population response to the two CS+ odors became highly correlated after learning,  
179 whereas the population response to the CS+ and CS- odors became less correlated  
180 (Figure 2E, 2F).

181

182         We performed decoding analysis to further examine the effect of learning on the  
183 OFC representation. A linear decoder trained on population responses prior to training  
184 decoded odor identity in the OFC at near chance levels (41% accuracy, chance is 25%).  
185 A decoder trained on population responses after learning distinguished between  
186 rewarded and unrewarded odors with greater than 95% accuracy (Figure 2G, S2F). In  
187 contrast, a decoder trained to distinguish between the identities of the two CS+ odors in  
188 OFC performed at close to chance level (Figure 2H, S2F). A decoder also failed to  
189 distinguish between the identities of the two CS- odors after learning (Figure 2I, S2F).

190 This is in accord with our observation that the population activities between the two CS+  
191 odors are highly correlated. These data suggest that the representation of odor identity  
192 encoded in piriform is discarded in the OFC and transformed into a representation of  
193 positive value by learning.

194

### 195 **The OFC Representation Reflects Changes in Value**

196 If the value of an odor changes, the representation of value in OFC should also  
197 change (Roesch et al., 2007; Schoenbaum et al., 1999; Thorpe et al., 1983). We  
198 therefore recorded the neural responses in OFC during reversal learning. Mice were  
199 first trained with 2 CS+ and 2 CS- odors in the appetitive learning task, and the odor  
200 reward contingencies were then reversed. After reversal, the mice displayed  
201 anticipatory licking to the old CS- odors (CS+ upon reversal) and suppressed  
202 anticipatory licking to the old CS+ odors (CS- upon reversal) after 30 trials (Figure S4A).  
203 Prior to reversal, imaging revealed that 30% of the neurons were more responsive to  
204 CS+ than CS- odors (Figure 3A, 3B, see STAR Methods). After reversal learning, 91%  
205 of CS+ responsive neurons diminished their response to the old CS+ odors, and 68% of  
206 these neurons were now activated by the new CS+ odors (S4B, S4C). As a  
207 consequence, 28% of OFC neurons are now more responsive to the new CS+ than CS-  
208 odors (Figure 3B, S3B). We also analyzed the strength of the odor-evoked responses  
209 during reversal learning at the level of neuronal populations. The response power to the  
210 old CS+ odors diminished three-fold upon reversal (Figure 3C, 3D, green) whereas the  
211 response power to the old CS- odors increased three-fold upon reversal (Figure 3C, 3D,  
212 red). The observation that the same cells diminished their responses to the old CS+

213 odors and responded to the new CS+ odors after reversal (Figure 3A, S4B, S4C)  
214 indicates that these neurons encode value rather than odor identity.

215

216 The value of a sensory stimulus should be contingent on internal state and  
217 context (Allen et al., 2019; Critchley and Rolls, 1996). CS+ odors predict water reward,  
218 an outcome of value to a thirsty mouse but of diminished value to a water-sated mouse.  
219 We therefore asked whether the representation of CS+ odors in OFC differs in thirsty  
220 and satiated mice. After appetitive learning, the mice were provided water. After  
221 satiation, the mice no longer displayed anticipatory licking to CS+ odors and rarely  
222 collect water when it is delivered (licking in less than 10% of trials) (Figure S4D).  
223 Imaging in the OFC revealed that prior to satiation, 30% of neurons responded to CS+,  
224 but 95% of these neurons were either no longer responsive or were significantly  
225 attenuated after satiation (Figure 3E, S3A). At a population level, the response power to  
226 the CS+ odors was more than 2.5-fold higher in thirsty mice (Figure 3F).

227

228 We also imaged mice for which the behavioral context was altered by removal of  
229 the water port. Under these conditions, water is not obtainable, and the value of the  
230 CS+ odor is presumably eliminated. Removal of the water port suppressed anticipatory  
231 licking to CS+ odors in less than three odor presentations (video recordings during  
232 imaging). Neuronal responses to the CS+ odors were either eliminated or significantly  
233 attenuated in 81% of the CS+ responsive neurons (Figure 3G, S3C). The response  
234 power to the CS+ odors was more than two-fold higher before water port removal  
235 (Figure 3H). Thus, changes in internal state and context that diminished the value of

236 water reward correlated with a significant attenuation in the activity of the CS+  
237 ensemble, providing further evidence that this OFC representation encodes value.

238

### 239 **The Role of the OFC Representation in Associative Learning**

240 We next performed optogenetic silencing to ask whether the OFC contributes to  
241 the learning of an appetitive association. AAV encoding either halorhodopsin or the red-  
242 shifted halorhodopsin Jaws was injected bilaterally into OFC (Chuong et al., 2014;  
243 Gradinaru et al., 2008). Electrophysiological recording sessions using a 32-channel  
244 extracellular optrode array demonstrated that photostimulation results in over 4-fold  
245 inhibition in spontaneous activity in mice expressing Jaws and 8-fold inhibition in mice  
246 expressing halorhodopsin (Figure S5) (Royer et al., 2010). Silencing of OFC during  
247 training was initiated two seconds prior to odor delivery and extended for two seconds  
248 beyond the time of water delivery. Mice that experienced OFC inhibition exhibited  
249 significant learning deficits (Figure 4A-F). The 9 silenced mice either did not lick  
250 consistently to the CS+ odors or licked indiscriminately to CS+ and CS- odors, or both.  
251 The number of trials to criterion (anticipatory licking in over 80% of CS+ odor trials) was  
252 two-fold higher in OFC silenced mice than in control mice (Figure 4A, 4B). In addition,  
253 the number of trials required to suppress licking to CS- odors (anticipatory licking in less  
254 than 20% of CS- odor trials) was four-fold higher in OFC silenced mice than in control  
255 mice (Figure 4C, 4D). Moreover, 5 of 9 mice failed to reach criterion and were unable to  
256 discriminate between CS+ and CS- odors even after 100 presentations of each odor  
257 within 8-10 training sessions (Figure 4E). Both control and silenced mice exhibit robust  
258 licking upon water delivery, suggesting that mice with OFC inhibition were highly

259 motivated to acquire water reward (Figure 4F). Thus, the neural representation of  
260 predictive value in OFC participates in the efficient acquisition of appetitive associations.

261

## 262 **The OFC Representation Diminishes After Learning**

263 The CS+ representation in OFC was strongest after 3 to 4 days of training, a time  
264 when behavioral performance plateaus, but diminished at later times despite the  
265 persistence of learned behavior. We therefore performed imaging experiments in a new  
266 cohort of mice for longer periods extending up to 9 training sessions (Figure 4G, 4H).  
267 The response power of the CS+ representation was maximal at 3 to 4 days of training  
268 and declined to amplitudes observed prior to training after 6-9 days (Figure 4I). The  
269 observation that the CS+ representation in the OFC diminished whereas the behavior  
270 persisted suggests that OFC may participate in the acquisition of appetitive  
271 associations, but is no longer required after initial learning.

272

273 We considered the possibility that our olfactory association task may involve  
274 distinct phases of learning with only the initial phase dependent on OFC. We considered  
275 a behavioral model in which mice first learn that odor predicts water, and in a second  
276 phase of learning, acquire the ability to discriminate which odors predict reward. We  
277 therefore implemented a head-fixed associative learning task consisting of two phases,  
278 pre-training and discrimination (Figure 5A). This task is similar to learning paradigms in  
279 freely moving mice that require pre-training for task acquisition, but the role of specific  
280 brain regions in pre-training in these behavioral experiments has not been examined  
281 (Bissonette et al., 2008; Burke et al., 2008; Izquierdo et al., 2004; Schoenbaum et al.,

282 1999, 2002, 2003; Stalnaker et al., 2007). In the pre-training phase of our new task a  
283 single odor was paired with water delivery. After mice successfully learned that odor  
284 predicts reward, a discrimination phase was initiated in which two new CS+ and two CS-  
285 odors were presented. This two-phase learning paradigm was conducted in cohorts of  
286 mice that express either Jaws or YFP in neurons in the OFC. OFC silencing in mice  
287 expressing Jaws impaired learning in the pretraining phase, with anticipatory licking  
288 requiring an average of 89 trials compared with 57 trials required by control mice  
289 (Figure 5B, 5C).

290

291 We next examined the role of OFC in the discrimination phase of the two-phase  
292 odor learning task. Mice expressing either Jaws or YFP in the OFC were pretrained in  
293 the absence of inhibition. After mice have successfully learned that odor predicts  
294 reward, anticipatory licking was observed in response to both the CS+ and CS- odors at  
295 the start of training (Figure S6A-D). This suggests that, during pretraining with a single  
296 CS+ odor, mice learn to generalize, associating all odors with reward. Control mice  
297 enhanced licking to the CS+ odors after 10 trials and suppressed licking to the CS-  
298 odors after 25 trials (Figure 5D, 5E, gray). Photoillumination of the OFC during the  
299 discrimination phase in mice expressing Jaws did not impair discrimination learning.  
300 Licking to CS+ odors (Figure 5D) and suppression of licking to CS- odors (Figure 5E)  
301 were similar in silenced and control mice. These data suggest that during the pre-  
302 training phase mice learn a simple association between odor and reward that engages a  
303 neural representation of value in the OFC. Once this association is learned, the OFC is

304 no longer required and a second brain structure facilitates the subsequent learning  
305 necessary for discrimination.

306

### 307 **Associative Conditioning in Freely Moving Mice**

308 We also examined the role of the OFC during pretraining in a two-phase freely  
309 moving behavioral paradigm (Figure 5F). In this task, mice expressing halorhodopsin or  
310 YFP in the OFC were placed into an arena. Freely moving mice first learned an  
311 association between odor and water during pre-training in an average of 211 trials  
312 (Figure 7R, gray), far more trials than required in the head-fixed task. Photoillumination  
313 of the OFC severely impaired the ability of 3 of 5 mice expressing halorhodopsin to  
314 learn this task (Figure 5G). These mice failed to initiate trials after eight days of training  
315 (Figure 5G), whereas the remaining mice initiated trials but learned slower than controls  
316 (halorhodopsin: 365 trials, control: 211 trials,  $p=0.07$ , ranksum test). The release of  
317 inhibition in the OFC restored the ability to learn in 2 of the 3 severely impaired mice.  
318 Optrode recordings confirmed that photo-illumination results in a ten-fold inhibition of  
319 OFC neurons.

320

321 We next examined the consequence of OFC inactivation in the discrimination  
322 phase of the task. Freely moving mice expressing either halorhodopsin or YFP in the  
323 OFC were pretrained in the absence of inhibition and the OFC was inhibited during  
324 discrimination learning. As we observed in the head-fixed task, mice expressing YFP  
325 exhibited generalized anticipatory licking at the start of discrimination learning (Figure  
326 7S, 7U, gray). These control mice then suppressed licking to the CS- odor and

327 enhanced licking to the CS+ odor in under 60 trials (Figure 5H, 5I). Licking to CS+ odors  
328 (Figure 5H) and suppression of licking for CS- odors (Figure 5I) in silenced mice were  
329 similar to controls. The results of OFC inhibition in freely moving mice are in accord with  
330 our observations in the head-fixed paradigm and demonstrate that the OFC is important  
331 in learning an association between odor and water during pretraining, but once this  
332 knowledge is acquired the OFC is no longer necessary for discrimination learning.

333

### 334 **Temporal Representations in OFC in the Two-Phase Paradigm**

335 We performed imaging experiments to examine the relationship between odor  
336 representations in OFC and behavior in the two-phase head-fixed task. During  
337 pretraining, a strong CS+ representation emerges with 26% of the neurons responding  
338 to the pretraining CS+ odor (Figure 6A). Responses after training were more consistent  
339 and of higher amplitude than before training and the response power to the CS+ odor  
340 increased two-fold (Figure 6E). The properties of this representation are similar to that  
341 of the CS+ odors after learning in the single-phase task (Figure 2B). We then performed  
342 imaging during discrimination training, with mice exposed to two CS+ and two CS-  
343 odors. At the start of discrimination, 21% of the neurons were responsive to each of the  
344 four odors (Figure 6B). These responses were non-selective and weak in amplitude  
345 (Figure 6B, 6F, 6I). During discrimination training, neurons became selectively  
346 responsive to the CS+ odors (Figure 6C). Decoding analysis revealed that the CS+ and  
347 CS- ensembles were more separable after discrimination learning (decoder accuracy at  
348 onset of discrimination: 0.60, fully learned: 0.93, chance = 0.50) (Figure 6L). However,  
349 the response powers to CS+ and CS- odors were significantly weaker than the power to



350 the CS+ odor after pre-training. We continued to image the OFC for up to 4 days after  
351 discrimination learning plateaued. The CS+ representation gradually diminished, and  
352 the response power decreased to below the response to odors prior to training (Figure  
353 6D, 6H, 6K, S7A). Only 14% of the neurons responded to the CS+ odors and 11% of  
354 neurons responded to CS- odors after prolonged training. These imaging results are  
355 consistent with the behavioral observations. OFC is required to learn the association of  
356 the pre-training odor with water, and a rich representation of this odor is observed upon  
357 imaging. OFC is not required for discrimination learning during which its modest CS+  
358 representation weakens considerably. These results suggest that a second structure is  
359 employed to accomplish the task of discrimination learning.

360

### 361 **A Representation of Value in the mPFC**

362 Previous experiments have implicated the medial prefrontal cortex (mPFC) in  
363 reward learning (Birrell and Brown, 2000; Chudasama and Robbins, 2003; Kim et al.,  
364 2017; Kitamura et al., 2017; Ostlund and Balleine, 2005; Otis et al., 2017). We therefore  
365 performed imaging in the mPFC to discern whether a representation of value emerges  
366 during discrimination learning in the two-phase task that may support learning after the  
367 diminution of the OFC representation. Imaging of the mPFC during pretraining revealed  
368 that the response to the pretraining odor was sparse and of low amplitude, and did not  
369 increase with learning (Figure 7A, 7E). Mice were then exposed to two new CS+ and  
370 two CS- odors. After one day of discrimination training, we observed a significant  
371 response to all odors (Figure 7B, 7F, 7I). The population activities evoked by these  
372 odors were more correlated (Figure 7L, 7M) and of higher amplitude (Figure 7F, 7I) than

373 prior to training (Figure S7B), and may reflect the generalized licking to all odors (S6A-  
374 D).

375 As learning proceeds, we observed a population of neurons responsive only to  
376 CS+ odors (19%), accompanied by a second population responsive to CS- odors (22%)  
377 (Figure 7C). The CS+ and CS- representations increased in amplitude and became  
378 more separable during discrimination learning (Figure 7G, 7J, 7N). We continued to  
379 image the mPFC representation for up to 4 days after learning plateaued, and unlike the  
380 OFC representations, the mPFC ensembles remained robust and persistent (Figure 7D,  
381 7H, 7K). After prolonged training, 23% of mPFC neurons responded to CS+ odors, and  
382 a non-overlapping 25% of mPFC neurons responded to CS- odors (Figure 7D, 7O).  
383 These results are further supported by decoding analysis that revealed that the  
384 representations of CS+ and CS- odors are stable and separable after discrimination  
385 learning (Figure 7P).

386

387 We note that whereas we observe a robust CS+ response during discrimination  
388 learning, we do not observe a response to the CS+ odor during pretraining. This  
389 suggests that the emergence of a CS+ representation in mPFC during discrimination  
390 coincide with a requirement to distinguish between CS+ and CS- odors. Whatever the  
391 mechanism, the mPFC appears to transform a representation of odor identity encoded  
392 in piriform into two distinct and stable representations, a CS+ ensemble encoding  
393 positive value and a CS- ensemble encoding negative value.

394

395           We next examined the role of mPFC in the two-phase paradigm in freely moving  
396 mice. Mice expressing either halorhodopsin or YFP in the mPFC were photoilluminated  
397 during the different phases of the task. Inactivation of the mPFC during pretraining did  
398 not inhibit task performance (Figure 7Q, 7R), whereas silencing during discrimination  
399 impaired appetitive learning in response to CS+ odors. 91 trials on average were  
400 required to reach successful learning criterion to CS+ odors in mice (n=4) expressing  
401 halorhodopsin compared with 11 trials in control mice (n=21) expressing YFP (Figure  
402 7S, 7T). We note that control mice initiate licking in response to both CS+ and CS-  
403 odors at the start of discrimination (Figure 7S, 7U). In contrast, mPFC-silenced mice  
404 failed to lick at the onset of discrimination to all odors and slowly learned to lick in  
405 response to CS+ odors (Figure 7S, 7T), but not to CS- odors (Figure 7U, 7V). Silencing  
406 of the mPFC thus impaired both generalization and discrimination learning, but we do  
407 not know whether there is a causal relation between these two components of the  
408 behavior.

409

410           These data suggest that the neural representation in OFC during pre-training  
411 contributes to the learning of an association between odor and water. The OFC  
412 representation dissipated upon discrimination learning and a persistent representation  
413 of both CS+ and CS- odors emerged in the mPFC. The mPFC supports generalization  
414 and participated in the discrimination of odors predictive of reward, suggesting a  
415 transfer of information from OFC to mPFC in odor learning.

## 416 **DISCUSSION**

417           The representation of odor in piriform cortex is distributive and unstructured and  
418 cannot inherently encode value (Illig and Haberly, 2003; Iurilli and Datta, 2017; Poo and  
419 Isaacson, 2009; Rennaker et al., 2007; Stettler and Axel, 2009; Sugai et al., 2005; Zhan  
420 and Luo, 2010). Value must therefore be imposed in downstream structures by  
421 experience or learning. We have examined the representation of odors in piriform cortex  
422 as well as in two downstream stations, OFC and mPFC, as mice performed an  
423 appetitive olfactory learning task. In piriform cortex we observed minor changes in  
424 neural activity unrelated to learning, suggesting that piriform encodes odor identity  
425 rather than odor value. In orbitofrontal cortex, 30% of the neurons acquired robust  
426 responses to conditioned stimuli after training and these responses were modulated by  
427 context and internal state. The representation in OFC, however, dissipated after  
428 learning and a more stable representation of both CS+ and CS- odors emerged in  
429 medial prefrontal cortex. Thus, the representation of odor identity in piriform is  
430 transformed into representations of value in both OFC and mPFC. Moreover, these two  
431 brain structures appear to function sequentially in the learning of appetitive  
432 associations.

433

### 434 **Representation of Odor Identity in Piriform Cortex**

435           The imposition of value upon neuronal populations is often reflected in changes  
436 in either the amplitude or the number of neurons responsive to a stimulus and results in  
437 an increase in the sensitivity of the organism to conditioned stimuli (Buonomano and  
438 Merzenich, 1998). We observed minor changes in the amplitude and size of neural

439 ensembles responsive to odors during learning in the piriform. Associative learning  
440 could also alter the representation of a stimulus in a manner that enhances  
441 discrimination (Feldman, 2009). Odor ensembles were slightly more separable upon  
442 learning but these changes were qualitatively similar for both CS+ and CS- odors and  
443 were also observed upon passive odor exposure. These data suggest that changes  
444 in neural populations reflective of value must occur downstream of the piriform cortex.

445

446         The imposition of value downstream of piriform may be important to assure the  
447 specificity of behavioral output elicited by salient odors (Choi et al., 2011). Imposing  
448 value in piriform would result in the modification of outputs to all of piriform's  
449 downstream targets, which could drive multiple behavioral outputs. Value encoded  
450 downstream, however, affords a specificity of output that is difficult to achieve if  
451 reinforcement is imposed at the level of an odor representation in primary olfactory  
452 cortex. In addition, were value imposed in piriform cortex, the gating of value by internal  
453 state or external context would limit the perception of odor to subsets of states and  
454 contexts. Finally, changes in the weights of either bulbar inputs or associative  
455 connections between pyramidal neurons reflective of value could reduce the  
456 dimensionality of the odor representation in piriform. Thus, the imposition of value in  
457 downstream areas allows the piriform to maintain a high-dimensional representation of  
458 odor information that can support flexible and specific associations in multiple  
459 downstream regions.

460

461 **Representations of Value in OFC and mPFC**

462           We observed that a representation of odor identity in piriform was discarded in  
463 the prefrontal cortex and was transformed into a representation of value in OFC and  
464 mPFC. After learning, neurons responsive to conditioned stimuli (CS+ odors) emerged  
465 in the OFC and these responses were strongly modulated by context and internal state.  
466 Distinct representations of CS+ as well as CS- odors subsequently emerged in mPFC.  
467 Moreover, silencing of either region of prefrontal cortex impaired different phases of the  
468 appetitive learning paradigm. In accord with our findings, a neural representation of  
469 rewarded auditory stimuli was identified in both OFC and mPFC, and silencing of these  
470 brain structures elicited deficits in the acquisition and expression of learned behavior  
471 (Namboodiri et al., 2019; Otis et al., 2017). Representations of conditioned stimuli have  
472 been described in multiple brain regions during an associative learning task similar to  
473 our behavioral paradigm (Allen et al., 2019; Kim et al., 2017; Namboodiri et al., 2019;  
474 Otis et al., 2017). It is perhaps not surprising that prediction of a reward essential for the  
475 survival of a thirsty animal would register in multiple brain regions. However, the  
476 functional and temporal relationships among the multiple representations and their  
477 individual contributions to learning were previously unclear.

478

479           We have implemented an associative learning task consisting of two phases,  
480 pretraining and discrimination, in an effort to disambiguate the contributions of OFC and  
481 mPFC to learning. In the pretraining phase a single odor was paired with water delivery.  
482 After mice successfully learned that odor predicts reward, a discrimination phase was  
483 initiated in which the animals learned to distinguish CS+ from CS- odors. A  
484 representation of the CS+ odor emerged early in OFC during pretraining accompanied

485 by a weaker representation in mPFC. During the discrimination phase the CS+  
486 representation diminished in OFC, whereas representations of CS+ and CS- odors  
487 emerged in mPFC and remained stable long after learning. Moreover, silencing of OFC  
488 during the pretraining but not the discrimination phase impaired learning, whereas  
489 inactivation of mPFC during discrimination but not pretraining impaired learning. These  
490 observations suggest that during pretraining mice learn a simple association between  
491 odor and reward that engages a representation of value in OFC. Once this association  
492 is learned OFC is no longer required for subsequent odor discrimination and the  
493 representation in mPFC then facilitates the learning of associations necessary for  
494 discrimination.

495

496 Previous studies have concluded that lesions of OFC do not impair learning of  
497 appetitive associations (Burke et al., 2008; Chudasama and Robbins, 2003; Gallagher  
498 et al., 1999; Izquierdo et al., 2004; Ostlund and Balleine, 2007; Schoenbaum et al.,  
499 2002; Stalnaker et al., 2007). These studies also employed a two-phase conditioning  
500 task, but the consequence of lesioning of OFC during pretraining was not assessed.  
501 Similar to our observations, lesioning of OFC did not impair the discrimination phase of  
502 learning in these studies. A recent study that used a one-phase task observed that OFC  
503 inhibition impairs acquisition of learning, in agreement with our results (Namboodiri et  
504 al., 2019). Our studies disambiguate pretraining and discrimination and reveal the  
505 importance of OFC in the formation specific of associations between stimulus and  
506 reward.

507

## 508 **Representations of Value in Multiple Brain Regions**

509           One interpretation of our findings is that odor learning reinforces piriform inputs to  
510 OFC, activating a representation of value. OFC may then teach mPFC during  
511 discrimination by reinforcing piriform inputs to this brain structure. In this manner,  
512 parallel inputs from piriform to multiple downstream targets can be sequentially  
513 reinforced to generate multiple representations of odor value.

514

515           There are many potential explanations for the presence of multiple  
516 representations of value. Each representation, for example, may have subtly different  
517 functions resulting in components of cognitive or behavioral output that are not apparent  
518 in simple assays involving licking or freezing. The observation that OFC represents only  
519 CS+ responses whereas mPFC encodes both CS+ and CS- responses suggests that  
520 the two brain areas have distinct behavioral functions. OFC, for example, may impose  
521 value on odors, learning that odor predicts water, whereas odor memory, generalization,  
522 and the behavioral distinction between CS+ and CS- odors may require the mPFC.

523

524           The observation that the OFC representation precedes that of mPFC may reflect  
525 the transfer of information from OFC to mPFC. Contextual fear memory is also thought  
526 to require the transfer and consolidation of information. A salient context is initially  
527 thought to elicit a representation in CA1 of the hippocampus, which over time reinforces  
528 a contextual representation in mPFC (Bontempi et al., 1999; Goshen et al., 2011; Kim  
529 and Fanselow, 1992; Kitamura et al., 2017; Squire and Alvarez, 1995; Takehara-  
530 Nishiuchi and McNaughton, 2008). At early times after learning, behavior depends on



531 temporal lobe structures. Remote recall, however, depends on mPFC and no longer  
532 requires an active hippocampus. The persistence of remote contextual memories after  
533 bilateral hippocampal ablations argues for consolidation in cortex dependent upon a  
534 reinforcing teaching function mediated by the hippocampus.

535

536       Theoretical considerations also reveal advantages to encoding memories in  
537 multiple, partitioned brain structures (McClelland et al., 1995; Roxin and Fusi, 2013).  
538 The persistence of individual representations depends on the stability of synaptic  
539 reinforcement in different brain regions and may dictate their role in the learning  
540 process. Plastic synapses effecting fast learning can be rapidly overwritten, whereas  
541 less plastic synapses in different brain structures can stabilize memories (Benna and  
542 Fusi, 2016; Fusi et al., 2005; Roxin and Fusi, 2013). Whatever the advantage afforded  
543 by an early OFC representation, it must be transient because the ensemble of neurons  
544 encoding value dissipates while the mPFC representation emerges as a stable  
545 ensemble. The transient nature of the OFC population supports models in which OFC  
546 performs a teaching function during task acquisition, after which it is no longer required  
547 for learning discrimination or for the expression of the learned behavior.

548

#### 549 **The OFC Representation is Dependent on State and Context**

550       The ensembles in OFC exhibit features that suggest the incorporation of higher  
551 order cognitive information not apparent in the sensory representation in piriform cortex.  
552 We observed that both internal state and external context gated the value  
553 representation in the OFC. After learning, satiation or alterations in context (removal of

554 the water port) abolished the response to conditioned stimuli. Thus, piriform cortex  
555 represents the external world, i.e. the identity of an odor, whereas orbitofrontal and  
556 medial prefrontal cortex represent not only the external sensory world, but internal  
557 features: learning, context and state. This representation of value in OFC is dependent  
558 upon the coincidence of a conditioned stimulus, motivated internal state and appropriate  
559 context, and undoubtedly other internal factors that we have not explored. One simple  
560 model that incorporates these features invokes direct input of piriform neurons onto  
561 pyramidal cells in OFC. OFC neurons may also receive inhibitory inputs that prevent the  
562 animal from seeking water when the animal is satiated, and these inhibitory inputs may  
563 be disinhibited when the animal is in a thirsty state and in the appropriate context. This  
564 model affords a flexibility whereby the same neurons in OFC can represent input from  
565 multiple sensory modalities encoding values of distinct valence and gated by different  
566 states or contexts.

567

### 568 **Distinct CS+ and CS- Representations in mPFC**

569 Distinct CS+ and CS- representations in mPFC emerged after discrimination  
570 learning. The discrimination task we have employed has only two behavioral outcomes:  
571 lick or no lick. An explicit representation of each behavioral outcome will likely improve  
572 the accuracy of discrimination and may confer flexible responses to changes in stimulus  
573 value (Kim et al., 2017). The maintenance of a CS- representation may additionally  
574 prevent unlearning when stimulus value changes. Consider a scenario in which a  
575 stimulus of positive predictive value no longer predicts reward, and reward is provided  
576 once again at a remote time. Experiments on this extinction paradigm reveal that

577 relearning occurred considerably faster than learning a new association with a naïve  
578 odor (Bouton, 2004). This suggests that a CS+ representation persists after extinction  
579 and provides a stored but silent record of early but extinguished learning. Upon  
580 extinction a new CS- representation may emerge for a prior CS+ odor. This CS-  
581 representation may be dominant over the persistent CS+ representation to suppress  
582 licking. Behavioral extinction will be observed despite the persistence of a positive value  
583 representation in mPFC. Thus, the presence of distinct CS+ and CS- representation  
584 affords the organism flexible responses in a world of changing value.

585

### 586 **The Generation of Distinct CS+ and CS- Representations**

587         How do representations of CS- and CS+ odors arise in distinct populations of  
588 cells in the mPFC? In one model, during pretraining, animals exposed to a single CS+  
589 may learn that odor predicts reward through the emergence of a CS+ representation in  
590 the OFC. This CS+ representation in OFC may serve a teaching function in the mPFC  
591 at the initiation of discrimination learning and reinforce all piriform inputs onto the  
592 mPFC. Early in discrimination learning, all odors will therefore activate the mPFC CS+  
593 ensemble and drive generalized licking behavior. When the animals experience odors  
594 that are not associated with reward (CS-) a negative reward prediction error (RPE)  
595 signal may be generated by the failure of these odors to predict reward (Schultz, 2016).  
596 This negative RPE signal is then relayed onto the mPFC to drive the formation of a CS-  
597 ensemble in mPFC, distinct from the CS+ ensemble. In this manner, CS- odors will  
598 activate a distinct population of neurons in the mPFC that signals negative value. This  
599 model invokes the presence of cognitive representations of odor in at least three

600 different brain regions, each contributing a different component function that ultimately  
601 leads to stable, yet flexible memory of stimulus value.

602 **ACKNOWLEDGMENTS**

603 We thank Cory Root for experimental help with imaging; Abby Zadina, Kristen Lawlor,  
604 Yijing Chen, and Matthew Chin for technical assistance; Fabio Stefanini for guidance  
605 with decoding; Walter Fischler, Stefano Fusi, Rui Costa, Sandeep Datta, Daniel  
606 Salzman, Ashok Litwin-Kumar and members of the Axel and Abbott laboratories for  
607 discussions; and Clay Eccard for assistance in the preparation of the manuscript. This  
608 work is supported by the Columbia Neurobiology and Behavior Program (P.Y.W.), the  
609 Helen Hay Whitney Foundation (C.B.), Simons Foundation (L.F.A and R.A.), NSF  
610 NeuroNex Award DBI-1707398 and the Gatsby Charitable Foundation (L.F.A), and the  
611 Howard Hughes Medical Institute (R.A.). R.A. is an HHMI investigator.

612 **AUTHOR CONTRIBUTIONS**

613 P.Y.W, C.B., L.F.A. and R.A. conceived the project, participated in its development and  
614 wrote the paper. P.Y.W., C.B., and N.P.S. performed the behavioral experiments and  
615 optogenetic manipulations. P.Y.W performed the imaging experiments and data  
616 analysis. P.Y.W, W.Z. and P.S. performed optrode experiments.

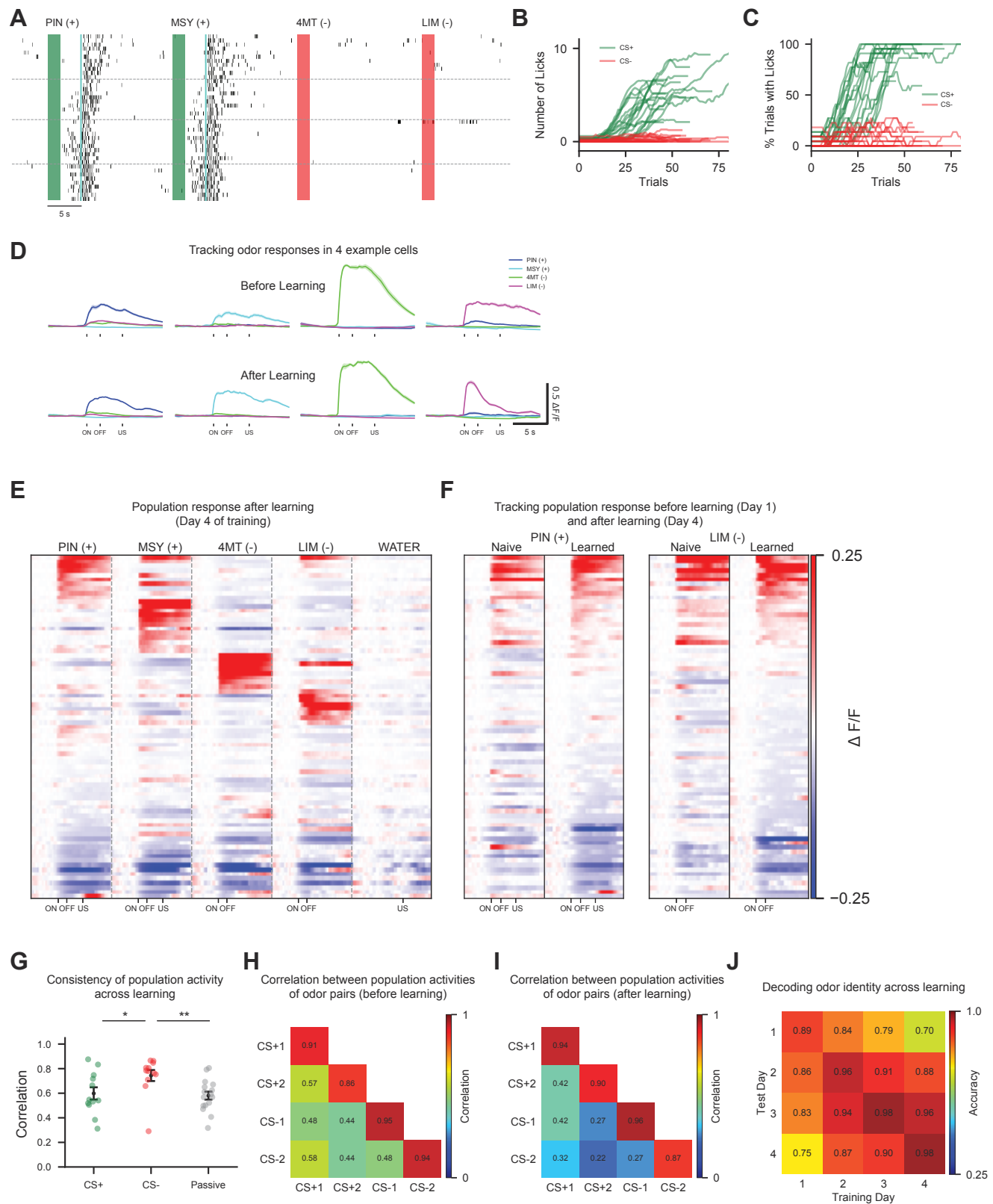
617 **DECLARATION OF INTERESTS**

618 The authors declare no competing interests.

619 **FIGURES**

620





621 **Figure 1. Odor representations in piriform cortex are stable during learning.**

622 (A) Anticipatory licking behavior in response to CS+ (green) but not CS- (red) odors  
623 after learning. Odor was presented for two seconds (green/red bars), followed by a  
624 three second delay before water delivery. Black rasters denote single lick events.

625 Horizontal lines denote the 4 training sessions. Odors: PIN: pinene (CS+), MSY: methyl  
626 salicylate (CS+), 4MT: 4-methylthiazole (CS-), LIM: limonene (CS-).

627 (B and C) Summary of training data for the appetitive odor discrimination task (n = 19  
628 mice, combined across multiple imaging and behavioral experiments). Number of  
629 anticipatory licks (B) and percentage of trials with anticipatory licking (C) to CS+ and  
630 CS- odors. Green lines represent an average of the two CS+ odor trials for a single  
631 mouse and red lines represent averages of the two CS- odor trials for a single mouse.

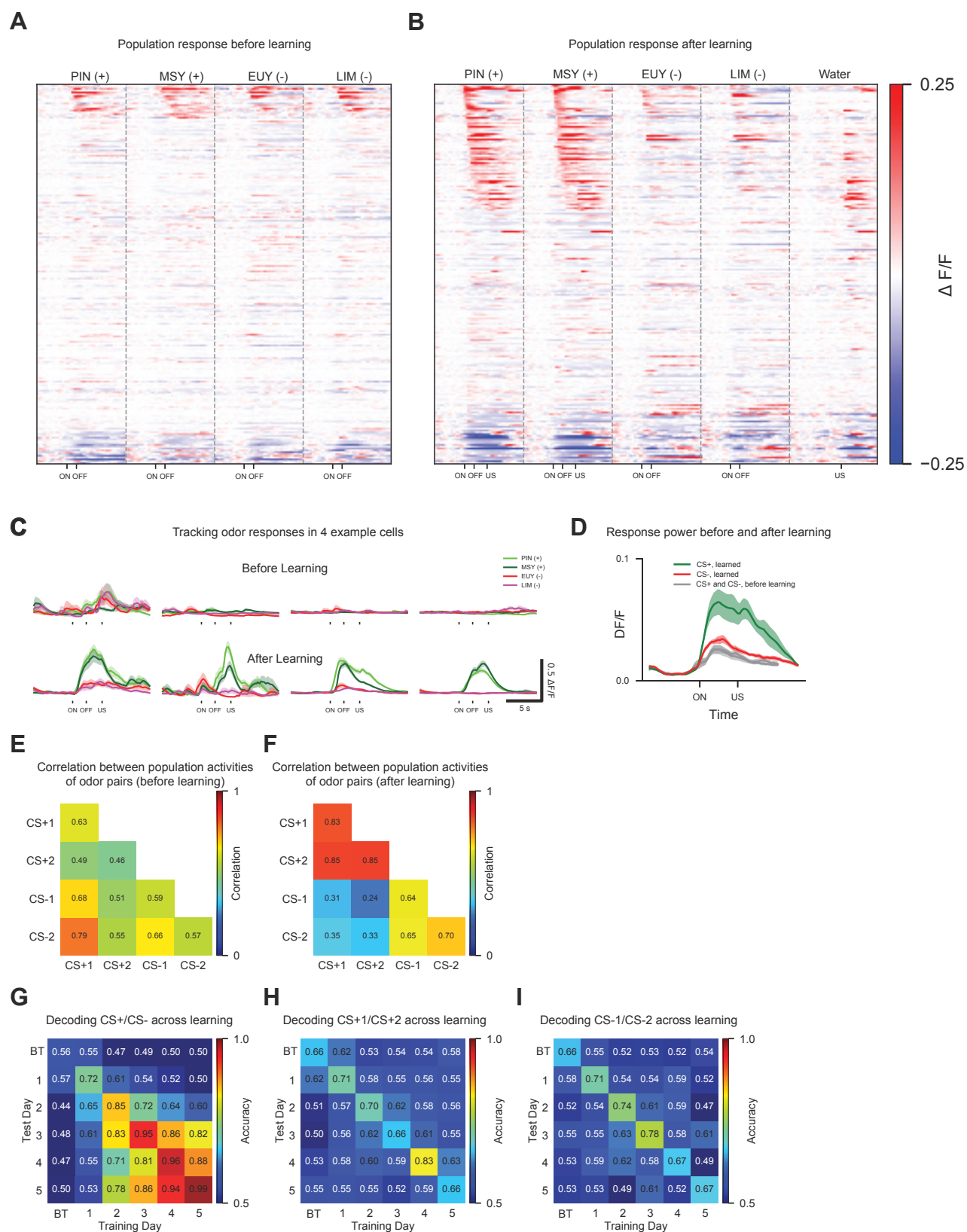
632 (D) Trial-averaged responses of 4 example piriform neurons to odors before learning  
633 (top, day 1 of training) and after learning (bottom, day 4 of training). ON: odor onset.  
634 OFF: odor offset. US: water delivery. Shading indicates  $\pm 1$  SEM.

635 (E) PSTH of piriform responses for one mouse. Cells are sorted by response amplitude  
636 to each of the 4 odors. Each row denotes a single cell's trial-averaged responses to the  
637 four odors and water. For all PSTH plots, mean activity during the baseline period (5  
638 seconds prior to odor delivery) is subtracted from each cell. See STAR Methods.

639 (F) PSTH before learning and after learning for PIN (CS+) and LIM (CS-) from the same  
640 mouse as in (E). For each odor, responses are aligned across days and sorted by  
641 evoked amplitude after learning.

642 (G) Pearson correlation was calculated between vectors encoding odor-evoked  
643 population activity before learning (day 1 of training) vs. after learning (day 4 of training),

644 and day 1 vs. day 4 of passive odor exposure. Each dot represents across-day  
645 correlations for a single odor in one mouse. Correlation values were: CS+: 0.60, CS-:  
646 0.74, passive: 0.58. N = 6 mice for odor learning, N = 4 mice for passive odor exposure.  
647 Green: CS+ odors. Red: CS- odors. Gray: passive. \* P < 0.05, \*\* P < 0.01, Dunn's test  
648 for multiple comparisons. Error bars indicate mean  $\pm$ 1 SEM. See STAR Methods.  
649 (H and I) Correlation of activity evoked by all odor pairs before (H) and after (I) learning.  
650 Correlations are calculated using the population activities for all pairs of odors in a given  
651 day and are averaged across the 6 imaged mice. Average correlation for all pairs of  
652 distinct odors before learning: 0.50, after learning: 0.32, p < 0.001, Wilcoxon signed-  
653 rank test. Diagonal entries represent self-correlations calculated after splitting shuffled  
654 trials of a given odor into two equal halves. See STAR Methods.  
655 (J) Accuracy of decoding the identities of the four tested odors from population activity  
656 within and across training days. Chance accuracy is 25%. Before learning (train and test  
657 on day 1): 0.89, after learning (train and test on day 4): 0.98, p = 0.04, Wilcoxon signed-  
658 rank test. 40 randomly chosen neurons per animal were used and values shown were  
659 averaged across 100 repetitions and 6 imaged mice. See STAR Methods.  
660  
661 See also Figure S1.



662 **Figure 2. A CS+ representation emerges in the OFC after learning**

663 (A and B) PSTH of OFC responses for all imaged mice (n=5) before (A) and after (B)

664 learning. Odors: PIN: pinene (CS+), MSY: methyl salicylate (CS+), EUY: eucalyptol

665 (CS-), LIM: limonene (CS-). Responses before and after learning are not aligned but

666 sorted for each panel by response amplitude to CS+ odors. Due to differences in

667 experimental conditions, imaging data from 1 mouse could not be combined with the 4

668 other mice in (A), so 4 mice are shown in (A).

669 (C) Trial-averaged responses of 4 example OFC cells to odors before learning (top) and

670 after learning (bottom). ON: odor onset. OFF: odor offset. US: water delivery. Here and

671 below, shading indicates  $\pm 1$  SEM.

672 (D) Average response power of OFC neurons to CS+ and CS- odors before learning (all

673 odors: gray), and after learning (CS+: green, CS-: red). N=5 mice. See STAR Methods.

674 (E and F). Within-day correlations between odor ensembles before learning (E) and

675 after learning (F). Average correlation between the population activities evoked by CS+1

676 and CS+2 before learning: 0.49, after learning: 0.85,  $p = 0.04$ , Wilcoxon signed-rank

677 test. Correlation between all CS+/CS- odor pairs before learning: 0.63, after learning:

678 0.30,  $p < 0.001$ , Wilcoxon signed-rank test.

679 (G-I). Accuracy of decoding predictive value (CS+ odors vs. CS- odors, G), CS+ identity

680 (CS+1 vs. CS+2, H), and CS- identity (CS-1 vs. CS-2, I) from OFC population activity

681 within and across training days. 40 randomly chosen neurons per animal were used.

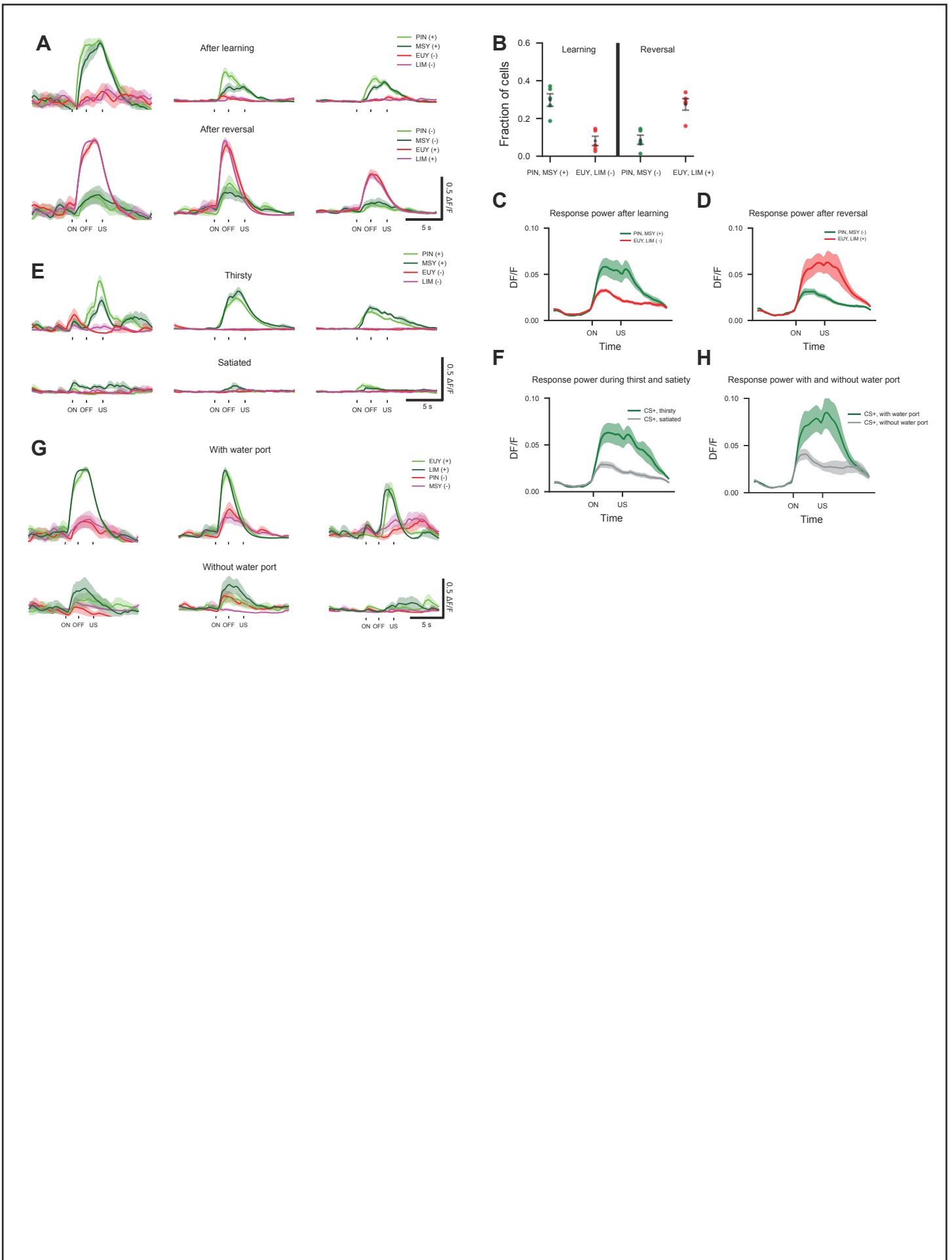
682 Values shown are averaged across 100 repetitions and 5 imaged mice. Chance

683 accuracy is 50% for all three conditions. BT: before training.

684

685 See also Figure S2 and S3.

686



687 **Figure 3. The CS+ representation in OFC is sensitive to internal state and external**  
688 **context**

689 (A) Trial-averaged responses of 3 example OFC cells after learning (top) and after  
690 reversal (bottom). PIN and MSY (CS+) were rewarded during discrimination learning,  
691 but not during reversal. EUY and LIM (CS-) were not rewarded during discrimination  
692 learning, but were rewarded during reversal. Here and below, shading indicates  $\pm 1$   
693 SEM.

694 (B) Fraction of neurons that are more responsive either to CS+ or to CS- odors after  
695 learning and after reversal for 5 mice. After learning CS+: 0.30, CS-: 0.08. After reversal  
696 CS+: 0.09, CS-: 0.27. Error bars indicate mean  $\pm 1$  SEM and dots indicate individual  
697 animals. See STAR Methods.

698 (C and D) Average response power of OFC neurons to CS+ (green) and CS- (red)  
699 odors after learning (C) and after reversal (D).

700 (E) Trial-averaged responses of 3 example OFC cells in an animal that was thirsty (top)  
701 and then immediately satiated (bottom).

702 (F) Average response power of OFC population to CS+ odors in thirsty (green) and  
703 satiated mice (gray). N = 5 mice.

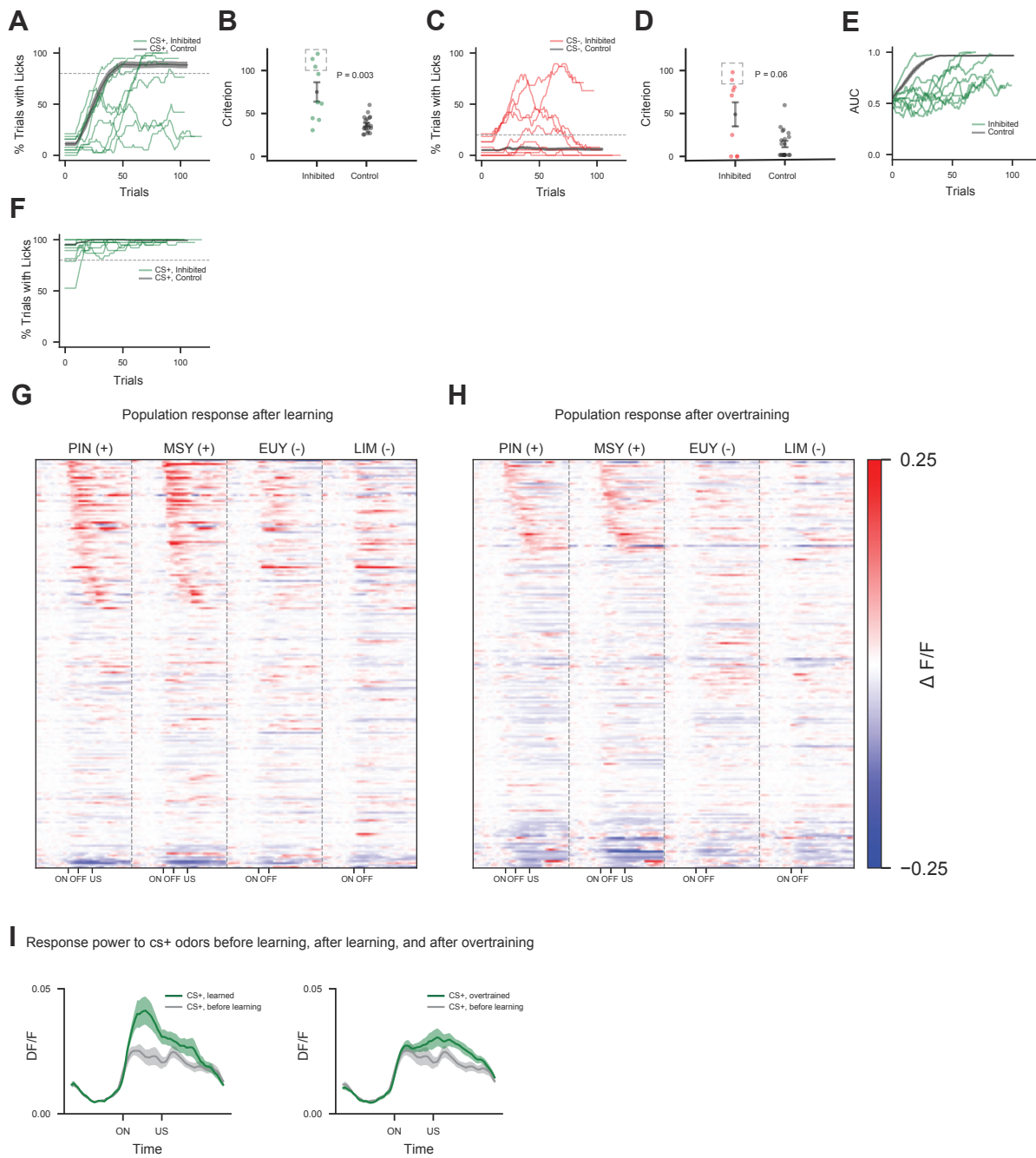
704 (G) Trial-averaged responses of 3 example cells when the water port was present (top)  
705 or absent (bottom).

706 (H) Average response power of OFC population to CS+ odor when water port was  
707 present (green) or absent (gray). N=4 mice.

708

709 See also Figure S3 and S4.





710 **Figure 4. OFC is necessary for associative learning and the odor representation**  
711 **in OFC peaks during learning but diminishes after over-training**

712 (A-F). Optogenetic silencing of OFC during appetitive learning. OFC inhibition (n=9  
713 mice) was accomplished with either mice expressing Jaws (n=4) or halorhodopsin  
714 (n=5). Control animals (n=19) are pooled across conditions. See STAR Methods for  
715 inhibition protocol.

716 (A) Fraction of trials with anticipatory licks to the CS+ odors. Dotted line indicates  
717 criterion for learning to lick to CS+ odors (>80% of trials with anticipatory licking). Here  
718 and below, shading indicates  $\pm 1$  SEM for control animals.

719 (B) Summary of trials to criterion for licking to CS+ odors in OFC silenced and control  
720 mice. Inhibited (green): 75 trials, control (gray): 37 trials,  $p = 0.003$ , ranksum test. Three  
721 inhibited mice did not reach criterion at the end of training (dotted square), and trials to  
722 criterion for these mice was defined as the last trial of training. Here and below, error  
723 bars indicate mean  $\pm 1$  SEM and dots indicate individual animals. See STAR Methods.

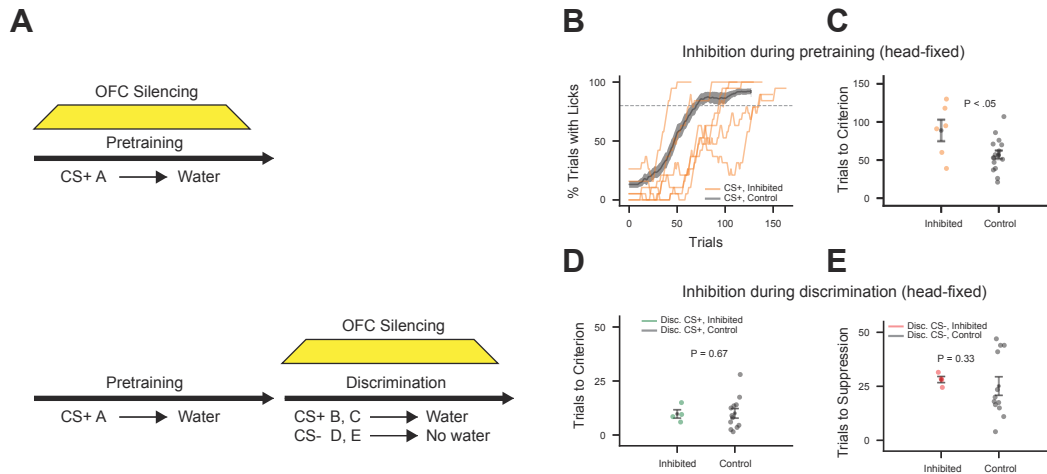
724 (C) Fraction of trials with anticipatory licks to the CS- odors. Dotted line indicates  
725 criterion for suppression of licking to CS- odors (<20% of trials with anticipatory licking).

726 (D) Summary of trials to criterion for suppression of licking to CS- odors in OFC silenced  
727 and control mice. Inhibited (red): 49 trials, control (gray): 13 trials,  $p = 0.06$ , ranksum  
728 test. Two inhibited mice did not reach criterion at the end of training (dotted square),  
729 and trials to criterion for these mice was defined as the last trial of training.

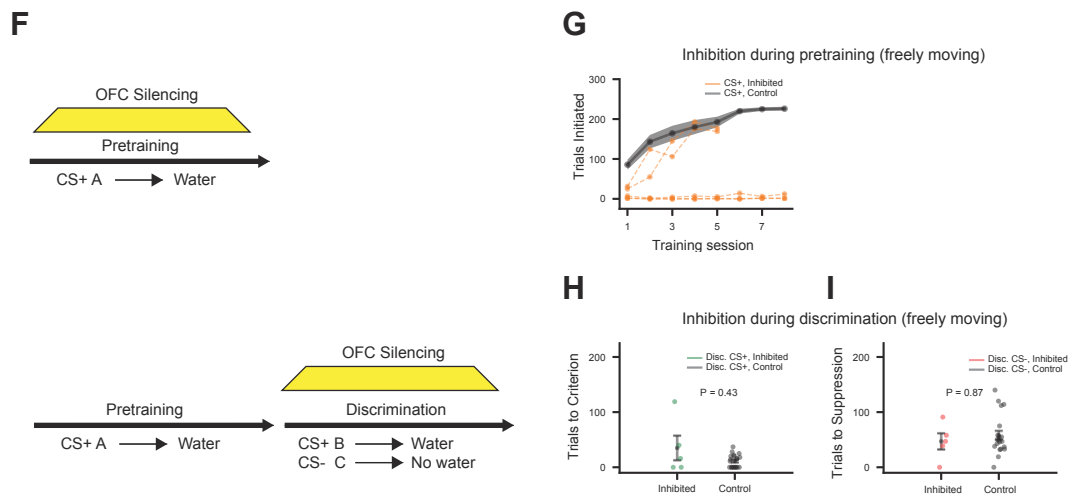
730 (E) Discriminability of licking to CS+ and CS- odors. AUC (area under ROC curve) was  
731 calculated by comparing the distribution of anticipatory licks in CS+ trials to that in CS-  
732 trials over a moving average window of 20 trials. An AUC of 0.5 indicates zero

733 discriminability between licks to CS+ and CS- odors; an AUC of 1.0 indicates complete  
734 discriminability with more licking to CS+ than CS- odors. Green: inhibited, gray: controls.  
735 (F) Percentage of trials with collection licks to CS+ (green) odors. Green: inhibited mice.  
736 Gray: control mice. Collection licks are defined as the number of licks during the 1  
737 second after water delivery.  
738 (G and H) PSTHs of OFC responses for all mice (n=3) to CS+ (PIN and MSY) and CS-  
739 (EUY and LIM) odors after learning (G) and after over-training (H). Responses after  
740 learning and after over-training are not aligned but sorted for each panel by response  
741 amplitude to CS+ odors.  
742 (I) Left: average response power of OFC neurons to CS+ odors before learning (grey)  
743 and after learning (green). Right: before learning (grey) and after over-training (green).  
744  
745 See also Figure S5.  
746

### Head-Fixed



### Freely Moving



747 **Figure 5. OFC is necessary for initial learning**

748 (A) Schematic of optogenetic silencing of OFC in a head-fixed task.

749 (B and C) OFC silencing during the pre-training phase of the two-phase task in head-  
750 fixed mice. Mice expressing Jaws: n=6, control mice: n=16. Control animals are pooled  
751 across conditions (see STAR Methods).

752 (B) Percentage of trials with anticipatory licks to the pretraining CS+ odor (Mice  
753 expressing Jaws: orange, control: gray). Here and below, shading indicates  $\pm 1$  SEM for  
754 control animals.

755 (C) Trials to criterion for licking to the pretraining CS+ odor. Mice expressing Jaws  
756 (orange): 89 trials, control (gray): 57 trials,  $p = 0.04$ , ranksum test. Here and below,  
757 error bars indicate mean  $\pm 1$  SEM and dots indicate individual animals.

758 (D and E) OFC silencing during the discrimination phase of the two-phase task in head-  
759 fixed mice. Mice expressing Jaws: n=4, control mice: n= 12.

760 (D) Trials to criterion for licking to CS+ odors. Mice expressing Jaws (green): 10 trials,  
761 controls (gray): 10 trials,  $p=0.67$ , ranksum test.

762 (E) Trials to criterion for suppression of licking to CS- odors. Mice expressing Jaws  
763 (red): 25 trials, controls (gray): 28 trials,  $p = 0.33$ , ranksum test. We noted that mice  
764 expressing Jaws rapidly learned to suppress licking to CS- odors after 15 trials on the  
765 first day of discrimination training but may have a deficit in memory.

766 (F) Schematic of optogenetic silencing in a freely moving task.

767 (G) OFC silencing during the pre-training phase of the two-phase task in freely moving  
768 mice. Mice expressing halorhodopsin: n=5, orange; mice expressing YFP: n=21, gray.  
769 YFP animals are pooled across conditions. Number of trials initiated during pre-training

770 is plotted as a function of training days. 3 of 5 mice with OFC inhibition failed to initiate  
771 trials.

772 (H and I) Same as D, E for freely moving animals. Mice expressing halorhodopsin: n=5,  
773 mice expressing YFP: n= 21.

774 (H) Trials to criterion for licking to CS+ odors. Mice expressing halorhodopsin (green):  
775 35 trials, mice expressing YFP (gray): 11 trials,  $p=0.43$ , ranksum test.

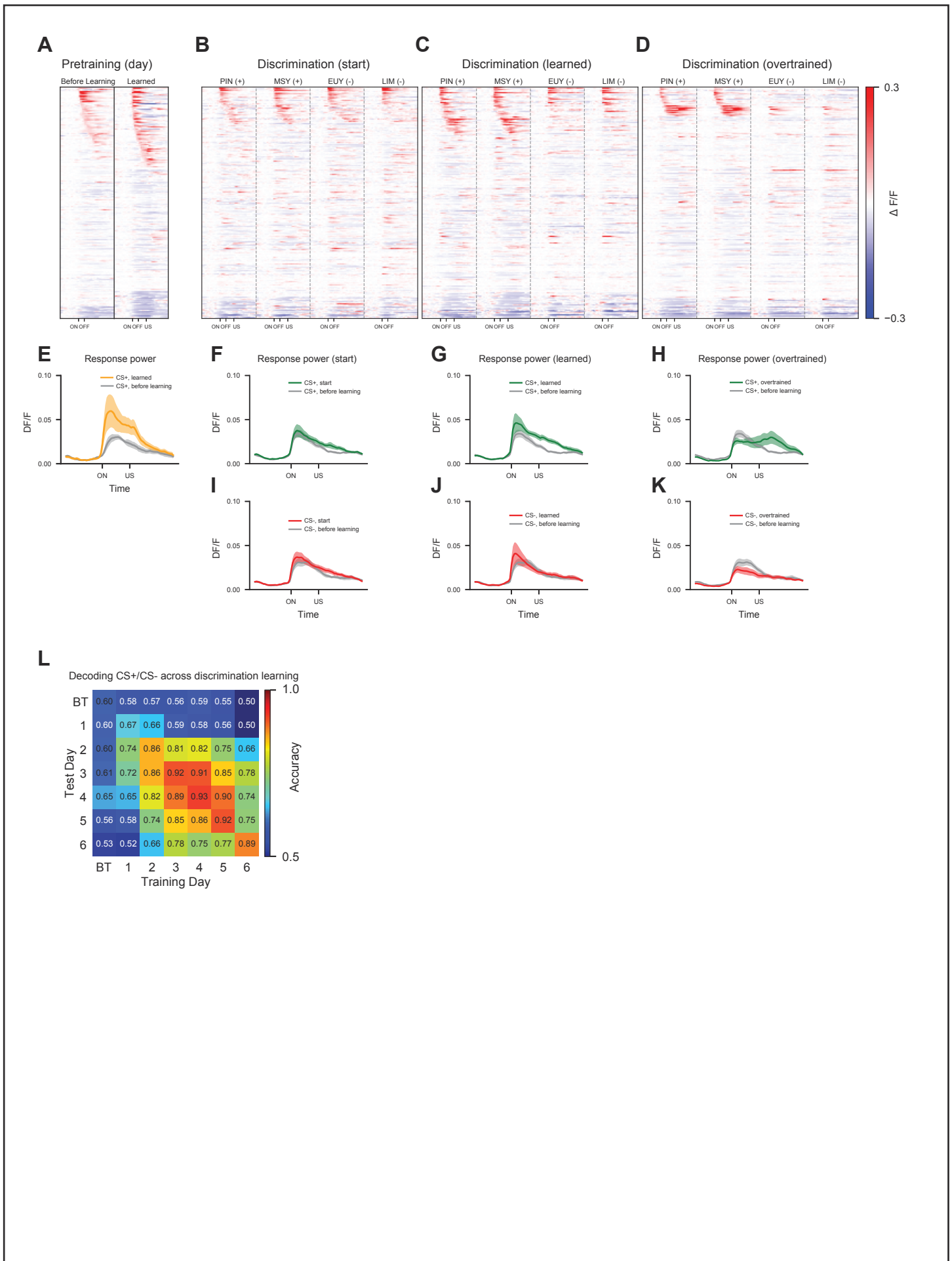
776 (I) Trials to criterion for suppression of licking to CS- odors. Mice expressing  
777 halorhodopsin (red): 47 trials, mice expressing YFP (gray): 58 trials,  $p = 0.87$ , ranksum  
778 test.

779

780 See also Figure S6.

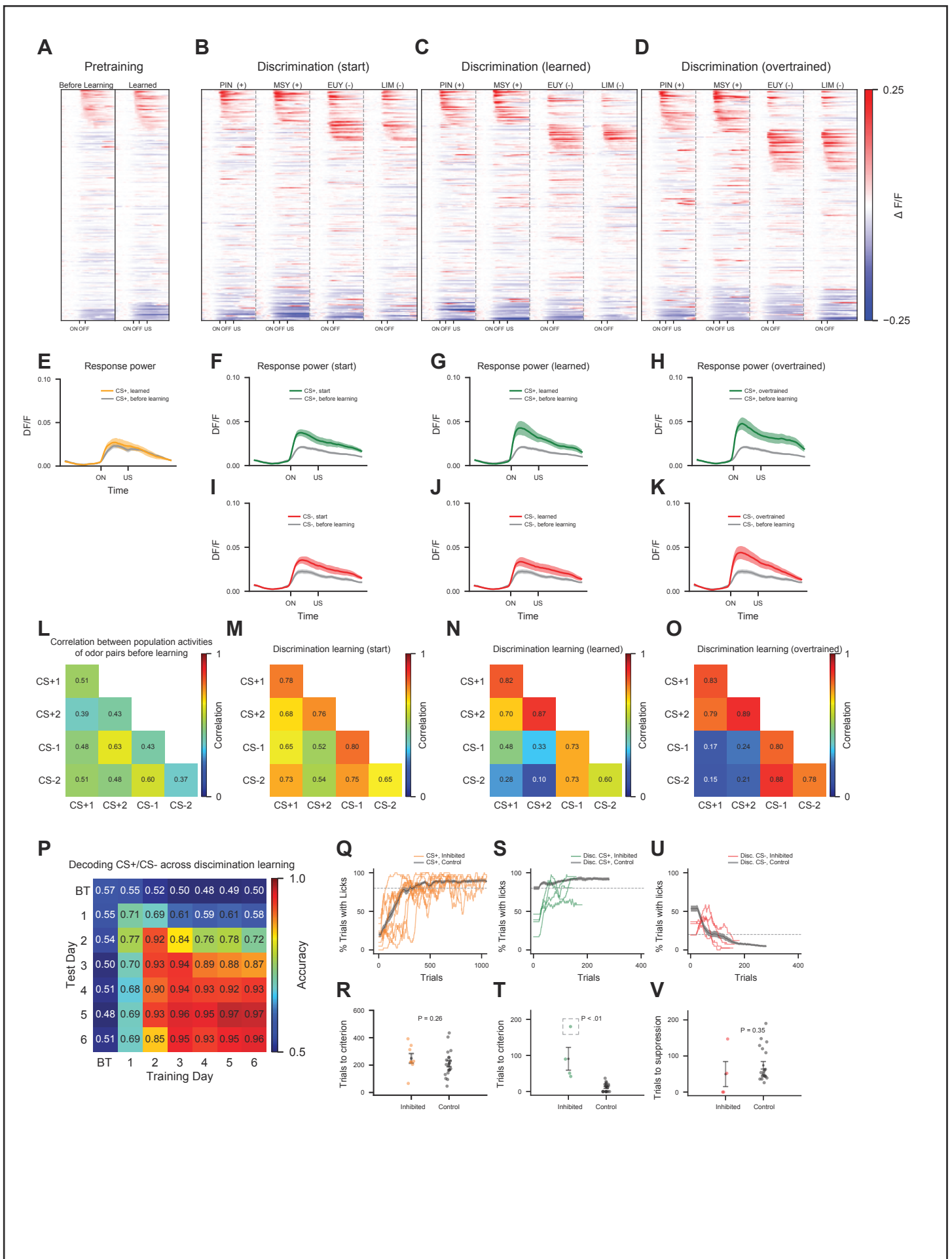
781

782



783 **Figure 6. The odor representation in OFC peaks during pretraining and**  
784 **diminishes during discrimination learning**  
785 (A-D) PSTH of OFC responses during multiple days of the two-phase task for all mice  
786 (n=4). Responses on different days are not aligned but sorted individually.  
787 (A) Responses to the CS+ odor (3-octanol) during the pretraining phase before (day 1)  
788 and after learning (day 3).  
789 (B-D) Responses to 2 new CS+ and 2 CS- odors after the first day of discrimination  
790 training (B), after discrimination learning (C), and after over-training (D).  
791 (E) Response power of the OFC representation to the CS+ odor before pretraining  
792 (gray) and after pretraining (orange). Here and below, shading indicates  $\pm 1$  SEM.  
793 (F-H) CS+ response power on the first day of discrimination learning (F), after  
794 discrimination learning (G), and after over-training (H). Average response power evoked  
795 by the two CS+ odors during each of these periods (green) is compared to the response  
796 power evoked by the same odors prior to training (gray).  
797 (I-K) CS- response power on the first day of discrimination learning (I), after  
798 discrimination learning (J), and after over-training (K). Average response power evoked  
799 by the two CS- odors during each of these periods (red) is compared to the response  
800 power evoked by the same odor prior to training (gray).  
801 (L) Accuracy of decoding predictive value (CS+ odors vs. CS- odors) from OFC  
802 population activity within and across days of discrimination training. 40 randomly chosen  
803 neurons per animal were used. Chance accuracy is 50%. BT: before training (naïve  
804 odors). Indices for days start after 3-4 days of pretraining has concluded.  
805  
806 See also Figure S7.





807 **Figure 7. CS+ and CS- representations emerge in mPFC during discrimination and**  
808 **mPFC is required for discrimination learning**

809 (A-D) PSTH of mPFC responses during multiple days of the two-phase task for all mice  
810 (n=4). Responses on different days are not aligned but sorted individually.

811 (A) Responses to the CS+ odor during the pretraining phase before and after learning.

812 (B-D) Responses to 2 new CS+ and 2 CS- odors after the first day of discrimination  
813 training (B), after discrimination learning (C), and after over-training (D).

814 (E) CS+ response power before pretraining (gray) and after pretraining (orange). Here  
815 and below, shading indicates  $\pm 1$  SEM.

816 (F-H) CS+ response power on the first day of discrimination learning (F), after  
817 discrimination learning (G), and after over-training (H). Average response power evoked  
818 by the two CS+ odors during each of these periods (green) is compared to the response  
819 power evoked by the same odor prior to training (gray).

820 (I-K) CS- response power on the first day of discrimination learning (I), after  
821 discrimination learning (J), and after over-training (K). Average response power evoked  
822 by the two CS- odors during each of these periods (red) is compared to the response  
823 power evoked by the same odor prior to training (gray).

824 (L-O) Within-day correlations between the population activities for all pairs of odors prior  
825 to training (L), after the first day of discrimination training (M), after discrimination  
826 learning (N), and after over-training (O). Correlation between all pairs of distinct odors  
827 before learning (L): 0.52; start of discrimination training (M): 0.64,  $p = 0.014$ , Wilcoxon  
828 signed-rank test. Correlation between all CS+/CS- odor pairs at start of discrimination  
829 training: 0.61, after learning: 0.30,  $p < 0.001$ , Wilcoxon signed-rank test.

830 (P) Accuracy of decoding of predictive value (CS+ odors vs. CS- odors) from mPFC  
831 population activity within and across days of discrimination training. 40 randomly chosen  
832 neurons per animal were used. Chance accuracy is 50%. BT: before training. Indices for  
833 days start after 3-4 days of pretraining has concluded.

834 (Q-R) mPFC silencing during the pre-training phase of the two-phase task in freely  
835 moving animals. Mice expressing halorhodopsin: n= 8; mice expressing YFP: n= 21.  
836 YFP mice are pooled across conditions.

837 (Q) Percentage of trials with anticipatory licking to the pretraining CS+ odor (mice  
838 expressing halorhodopsin: orange, mice expressing YFP: gray). Here and below,  
839 shading indicates  $\pm 1$  SEM for control animals.

840 (R) Trials to criterion for licking to the pretraining CS+ odor. Mice expressing  
841 halorhodopsin (orange): 249 trials, mice expressing YFP (gray): 211 trials,  $p = 0.26$ ,  
842 ranksum test. Here and below, error bars indicate mean  $\pm 1$  SEM and dots indicate  
843 individual animals.

844 (S-V) mPFC inhibition during the discrimination phase of the two-phase task in freely  
845 moving animals. Mice expressing halorhodopsin: n= 4, mice expressing YFP: n= 21.

846 (S) Percentage of trials with anticipatory licking to the CS+ odor (mice expressing  
847 halorhodopsin: green, mice expressing YFP: gray).

848 (T) Trials to criterion for licking to the CS+ odor. Mice expressing halorhodopsin (green):  
849 91 trials, mice expressing YFP (gray): 11 trials,  $p = 0.002$ , ranksum test. One inhibited  
850 mouse did not reach criterion at the end of training (dotted square), and trials to criterion  
851 for this mouse was defined as the last trial of training.

852 (U) Percentage of trials with anticipatory licking to the CS- odor (mice expressing  
853 halorhodopsin: red, mice expressing YFP: gray).

854 (V) Trials to criterion for suppression of licking to the CS- odor. Mice expressing  
855 halorhodopsin (red): 50 trials, mice expressing YFP (gray): 74 trials,  $p = 0.35$ , ranksum  
856 test.

857

858 See also Figure S7.

859

860 **STAR METHODS**

861

862 **KEY RESOURCES TABLE**

| <b>REAGENT OR RESOURCE</b>   | <b>SOURCE</b>                          | <b>IDENTIFIER</b>   |
|--|--|---|
| <b>Experimental Models: Organisms/Strains</b>                        |  |   |
| Mouse: wild type C57BL/6J  | Jackson Laboratory                     | 000664  |
| Mouse: rosa26-loxp-stop-loxp-GCaMP6s                                 | Jackson Laboratory                     | 024106  |
| Mouse: Vglut2-ires-cre   | Jackson Laboratory                     | 016963  |
| <b>Other</b>   |  |   |
| 200 um, 0.39 NA optical fiber for optogenetics (mPFC)                | Thorlabs                               | Custom Fabrication  |
| 200 um, 0.39 NA optical fiber for optogenetics (OFC)                 | Thorlabs                               | CFM12L02  |
| 0.5-mm GRIN lens   | GRINTECH                               | NEM-050-50-00-920-S-1.5p  |
| <b>Software</b>  |  |   |
| MATLAB   | Mathworks                              | <a href="https://www.mathworks.com">Mathworks.com</a>   |
| MATLAB algorithm for registration within and across imaging sessions | <a href="#">Guizar-Sicairos et al.</a> | <a href="https://www.mathworks.com/matlabcentral/fileexchange/18401-efficient-subpixel-image-registration-by-cross-correlation">https://www.mathworks.com/matlabcentral/fileexchange/18401-efficient-subpixel-image-registration-by-cross-correlation</a> |
| MATLAB algorithm for extracting cellular CA <sup>+2</sup> signals    | <a href="#">Pnevmatikakis et al.</a>   | <a href="https://www.cell.com/neuron/fulltext/S0896-6273(15)01084-3">https://www.cell.com/neuron/fulltext/S0896-6273(15)01084-3</a>   |
| Custom MATLAB scripts for analyzing CA <sup>+2</sup> signals         | Mathworks                              | N/A   |
| FIJI   | University of Wisconsin-Madison LOCI   | <a href="http://fiji.sc/">http://fiji.sc/</a>   |
| Python 3.6   | Python                                 | <a href="https://www.python.org/">https://www.python.org/</a>   |
| Scikit-Learn   | <a href="#">Pedregosa et al.</a>       | <a href="https://scikit-learn.org/">https://scikit-learn.org/</a>   |
| iPython and Jupyter  | <a href="#">Perez et al.</a>           | <a href="https://jupyter.org">https://jupyter.org</a>   |

863

## 864 **CONTACT FOR REAGENT AND RESOURCE SHARING**

865 Further information and requests for resources and reagents should be directed  
866 to and will be fulfilled by the Lead Contact, Richard Axel (ra27@columbia.edu).

867

## 868 **EXPERIMENTAL MODEL AND SUBJECT DETAILS**

869 All experimental and surgical protocols were performed in accordance with the  
870 guide of Care and Use of Laboratory Animals (NIH) and were approved by the  
871 Institutional Animal Care and Use Committee at Columbia University. For all head-fixed  
872 behavior and inhibition experiments, Vglut2-ires-cre mice (Vong et al., 2011) were  
873 crossed to Ai96 (Madisen et al., 2015), and all male and female heterozygous  
874 transgenic offspring aged 8-16 weeks were used. For all freely-behaving behavior  
875 experiments, C57BL/6J mice aged 8-16 weeks were used. All animals were maintained  
876 under a normal 12 hour light/dark cycle with littermates until implantation of optical  
877 fibers or GRIN lenses.

878

## 879 **METHOD DETAILS**

### 880 **Stereotaxic Surgeries**

881 Mice were anesthetized with ketamine (100 mg/kg) and xylazine (10mg/kg)  
882 through intraperitoneal injection and then placed in a stereotactic frame. Body  
883 temperature was stabilized using a heating pad attached to a temperature controller.  
884 For lens implantation experiments, a 1.0-1.5mm round craniotomy centered on the  
885 implantation coordinate was made using a dental drill (see Table S1 for coordinates).  
886 Dura and 0.5mm – 1mm of underlying cortex was then aspirated. Blood was washed off

887 at the top constantly through aspiration. A 0.5mm diameter and 6.4 mm length  
888 microendoscope was then inserted. After implantation, the microendoscopes were fixed  
889 in place using Metabond (Parkell) onto the exposed region. To protect the lens that was  
890 protruding out of the skull from damage, a metal enclosure was placed around it (Dytran  
891 thread adapter) and covered with an acorn nut (Amazon). Lastly, a custom-made head  
892 plate (stainless steel) was attached to the skull with Metabond to allow for head-fixation.  
893

894 For optical fiber implantation experiments, virus was first injected using a  
895 micropipette that was made using a Sutter Micropipette Puller (P-2000). Volumes were  
896 injected at 100 nL per minute (see Table S4 for virus and injection information).  
897 Afterwards, 0.39-NA optical fibers (Thorlabs) were implanted bilaterally over the desired  
898 brain region. Following surgery, mice received buprenorphine (0.05 - 0.1 mg/kg)  
899 subcutaneously every 12 hours over the next three days. Mice recovered for at least 4  
900 weeks before the start of any imaging or optogenetic experiment.

901

## 902 **Animal Behavior**

903 For learning experiments, mice were water-restricted (water bottles taken out of  
904 cage) and received water (bottle placed back into cage) for 4-5 minutes every day.  
905 Behavioral training began when mice weighed less than 90% of free drinking weight (~3  
906 days for all experiments). Mice were also weighed every day to ensure good health. No  
907 health problems related to dehydration arose at any point.

908

## 909 ***Head-fixed behavior***



910 Mice did not undergo any form of shaping prior to assessment of a learning  
911 deficit during either the single-phase head-fixed learning task (Figure 4) or the pre-  
912 training phase of the two-phase head-fixed learning task (Figure 5). Mice were head-  
913 fixed on a large Styrofoam ball, where they could run freely in one axis (forwards and  
914 backwards). During imaging, mouse behavior was monitored with an IR camera (Point  
915 Grey). The custom olfactometer was made with mass flow controllers (Aarlborg) and  
916 quiet solenoid valves (Lee Company), which are controlled by a USB-DAQ  
917 (Measurement Computing) using high voltage transistor arrays. The odor stream was  
918 set to 800 mL/min, and split into two equal lines carrying 400 mL / minute (see Table S2  
919 for list of odorants used). One line was dedicated for odor detection by the animal. A  
920 narrow opening was placed next to the animal's nose to allow for odor sampling. The  
921 other line was routed to a photo-ionization device (Aurora Scientific) to measure odor  
922 ionization, an indicator of odor identity and concentration. Water was delivered through  
923 a quiet solenoid-controlled valve (Lee Instruments) to a water port (gavage needle).  
924 Licking events were collected through a capacitive touch sensor (Phidgets) attached to  
925 the water port. Behavioral training and data acquisition were accomplished with custom  
926 MATLAB scripts. All data was collected at 1000 Hz.

927

928 Most mice learned instantly, without any prior training, to lick from a water port to  
929 collect water. Each odor trial had the following structure: 5 seconds baseline, 2 seconds  
930 odor, 3 seconds delay, followed by water in the case of CS+ trials. The inter-trial interval  
931 was 25 seconds. During pre-training, only one CS+ odor was presented. In most  
932 experiments, octanol served as the CS+ odor during pre-training, and methyl salicylate

933 and pinene served as the CS+ odors, and eucalyptol and limonene served as CS-  
934 during discrimination learning. Each day of pre-training consisted of 40-60 trials of the  
935 single CS+ odor. Discrimination training consisted of five types of trials, delivered  
936 pseudo-randomly: 2 CS+ odors that predicted water delivery, 2 CS- odors, and US trials  
937 in which water was delivered without prior odor delivery. Each day of discrimination  
938 training consisted of 12-15 trials of each of the 5 conditions (60-75 trials total). For  
939 imaging experiments, most training sessions were conducted every other day to  
940 minimize GCaMP6S bleaching in transgenic mice.

941

942 For bilateral photo-inhibition experiments, a far-red laser (660 nm, CrystaLaser)  
943 was used for mice expressing the red-shifted halorhodopsin Jaws, and a 560 nm laser  
944 (CrystaLaser) was used for mice expressing the halorhodopsin NpHR. The laser was  
945 connected through a single patch cord and a rotary joint (Doric Lenses) to divide the  
946 laser output equally onto bilaterally implanted optical fibers. The power at the ends of  
947 each fiber tip was approximately 8-10 mW for all inhibition experiments. Laser was  
948 turned on 2 seconds prior to odor delivery and turned off 2 seconds after US delivery,  
949 lasting for a total of 9 seconds. Laser was also on for 9 seconds in CS- trials, beginning  
950 2 seconds before odor delivery. To confirm that the optical fibers had delivered the  
951 expected amount of power during the experiment, fiber implants were extracted  
952 immediately after perfusion and output power levels at the fiber tip was re-tested.  
953 Additionally, we included only mice in which viral expression within the target area of  
954 interest was robust after histological analysis. No mice were excluded based on these  
955 two criteria.

956

957 ***Freely-moving behavior***

958 Mice did not undergo any form of shaping prior to assessment of a learning  
959 deficit during the pre-training phase of the two-phase learning task (Figure 5, 7). Water-  
960 restricted animals were placed in a 1ft x 1ft training chamber and allowed to explore  
961 freely. The training chamber was placed in a sound-attenuating PVC cabinet  
962 (MedAssociates) and was retrofitted with a custom-made ceiling with a holder  
963 (Thorlabs) for a 1 to 2 rotary joint intensity splitter (Doric Lenses) that allowed free  
964 movement of the animal during laser photoillumination sessions. The training chamber  
965 had a built-in custom-made nose port on one wall. The nose port contained a lick spout  
966 (gavage needle) connected to a capacitive touch sensor (Phidgets), a vacuum line  
967 connected to wall vacuum and an odor line connected to the olfactometer. Training  
968 sessions took place in the dark and animals were monitored with an IR camera  
969 (Edmund Optics). All behavioral training was controlled with custom-written Python  
970 scripts. Entry of the animals' nose into the nose port was detected with IR sensors  
971 (Sparkfun). All behavioral training was controlled with custom-written Python scripts.

972

973 A behavioral training session lasted approximately 30 minutes and an animal  
974 could complete as many as 200 trials. For optogenetic silencing experiments, the laser  
975 was turned on for the entire training session. The laser output was divided equally to the  
976 bilaterally implanted ferrules through the rotary joint. The power was adjusted such that  
977 the power coming out of each fiber tip was 10-15 mW for all inhibition experiments.  
978 Odors (diluted to 1% with mineral oil) were pinene (CS+ during pre-training), isoamyl

979 acetate (CS+ during discrimination), and ethyl acetate (CS- during discrimination).  
980 Odors were delivered with a custom-made olfactometer (mass flow controllers,  
981 Aarlborg; quiet solenoid valves, Lee Company; USB-DAQ, National Instruments) and an  
982 air pump (MedAssociates) at a rate of 1 L/min. Trials of CS+ and CS- odors were  
983 delivered in a pseudo-random order. The trial structure was as follows: the trial was  
984 initiated when the animal inserted the nose into the nose port, as detected by the IR  
985 sensor. After 0.7 s, if the animal was still in the port (as reported by the IR sensor), the  
986 odor was delivered for 2.4 s, followed immediately by water if the odor was a CS+ odor.  
987 Each trial was followed by a 5 s inter-trial interval. Behavioral performance was  
988 quantified by measuring the percent of time spent licking in the 1.2 s interval before the  
989 end of odor delivery.

990

### 991 ***Head-fixed Imaging***

992 A two-photon microscope (Ultima, Bruker) was equipped with the following  
993 components to allow imaging of deep brain areas in vivo: a tunable mode-locked 2-  
994 photon laser (Chameleon Vision, Coherent) set to 920 nm, ~100 fs pulse width; a  
995 GaAsp-PMT photo-detector with adjustable voltage, gain, and offset feature  
996 (Hamamatsu Photonics); a single green/red NDD filter cube (580 dxxd dichroic,  
997 hq525/70 m-2p bandpass filter); a long working distance 10X air objective with 0.3 NA  
998 (Olympus).

999

1000 A 260 pixel X 260 pixel region of interest (~400 um X 400 um FOV) was chosen,  
1001 with 1.6 us dwell time per pixel, to allow image collection at 4.5 Hz. Imaging from of the

1002 same plane across multiple days (z-axis) was accomplished by using the top of the  
1003 GRIN lens as a reference point for alignment. For each trial, two-photon scanning was  
1004 triggered at the onset of the baseline period (5 seconds prior to odor delivery), and a 19  
1005 second (75 frames) video was collected. Data was acquired using custom acquisition  
1006 software (Bruker Instruments).

1007

### 1008 ***Optrode Experiments***

1009 Extracellular recordings were performed acutely in head-fixed animals using 32-  
1010 channel silicon probes (Buzsaki32, NeuroNexus) with a 100 um core fiber attached to  
1011 one of the four shanks. A 660 nm laser was used for Jaws activation and a 560nm laser  
1012 for Halorhodopsin activation (CrystaLaser). Recordings were performed 4 weeks after  
1013 virus injection. On recording days, mice were anesthetized with ketamine/xylazine and  
1014 the skull indentation created during virus injection was enlarged using a drill and the  
1015 dura was removed. Subsequently, mice were then head-fixed to the recording stage,  
1016 and the optrode was lowered inside the brain with a micro-manipulator. The incision  
1017 was then sealed with liquid agar (1.5%) applied at body temperature.

1018

1019 We lowered optical fibers down to 2-3 mm below Bregma towards the OFC and  
1020 performed a series of inhibition recordings with varying power levels (.5 mW, 1 mW, 2  
1021 mW, 5 mW, 10 mW, and 15 mW) at fiber tip. For each power level, the laser was turned  
1022 on for 10 seconds with an ITI of 30 seconds for a total of 15 consecutive blocks. In  
1023 Halorhodopsin-expressing animals, we also performed trials of 10 minutes of photo-  
1024 illumination to assess OFC silencing in a setting similar to the uninterrupted photo-

1025 illumination delivered throughout the entire training session in freely moving  
1026 experiments.

1027

1028 The 32-channel recording data were digitized at 40 KHz and acquired with  
1029 OmniPlex D system (Plexon Inc). The voltage signals were high-pass filtered (200 Hz,  
1030 Bessel) and sorted automatically with KlustaKwik (Rossant et al., 2016) or Kilosort  
1031 (Pachitariu et al., 2016). The clusters were then manually curated with KlustaViewa or  
1032 Phy GUI to merge spikes from the same units and to remove instances of noises and  
1033 units that were not well isolated. Spike data was converted into firing rates using a first-  
1034 order Savitzky-Golay filter with a smoothing window of 100 ms.

1035

### 1036 ***Histology***

1037 Mice were euthanized after anesthesia with ketamine/xylazine. Brains were  
1038 extracted and incubated in paraformaldehyde for 24 hours, and then coronal sections  
1039 (100um) were cut on a vibratome (Leica VT1000 S). The sections were then incubated  
1040 with far-red neurotrace (640/660, Thermo Fisher Scientific) to label neuronal cell bodies.  
1041 All images were taken using a Zeiss LSM-710 confocal microscope system. Histology  
1042 was performed to confirm locations of implanted lenses and optical fibers, as well as  
1043 expression levels for GCaMP6, YFP, Jaws, and Halorhodopsin.

1044

### 1045 ***Pooling Animal Cohorts Across Conditions***

1046 Animal cohorts A, B, C, and H were pooled as controls for OFC inhibition during  
1047 the single-phase discrimination learning task (see Tables S3 and S4 for cohort

1048 information). Animal cohorts D, E, J, and K were pooled as controls for OFC inhibition  
1049 during pretraining in the two-phase task. Animal cohorts D, E, and J were pooled as  
1050 controls for OFC inhibition during discrimination in the two-phase task. Animal cohorts  
1051 M, O, Q, and S were pooled as controls for inhibition experiments in all freely moving  
1052 two-phase tasks.

1053

#### 1054 ***Data Collection***

1055         Investigators were not blind during either imaging or optogenetic experiments.  
1056 For imaging experiments, mice were excluded if the field of view contained less than 20  
1057 neurons, if the signal was too dim, or if the lens was not placed directly above the region  
1058 of interest (n=1, Cohort C, Table S3). For optogenetic experiments, mice were excluded  
1059 if histology revealed low opsin expression within the region of interest, if the optic fibers  
1060 were not located at the targeted coordinate, or if the optic fibers did not transmit  
1061 excitation light properly (n=0, all conditions). 1 mouse was excluded from cohort R  
1062 because it failed to learn pretraining in the two-phase task in the absence of any  
1063 optogenetic silencing, and we therefore could not assess its performance during  
1064 subsequent discrimination learning (Table S4).

1065

#### 1066 **QUANTIFICATION AND STATISTICAL ANALYSIS**

1067         Image processing and calcium transient analysis were performed using  
1068 MATLAB. Significance was defined as  $p < 0.05$ . All statistical tests, behavioral data  
1069 analyses and imaging data analyses were performed using Python. Wilcoxon rank-sum

1070 test was used in two-group comparisons, Dunn's test was used for multiple-group  
1071 comparisons, and Wilcoxon signed-rank test was used in paired group comparisons.

1072

### 1073 ***Behavioral Data Analysis***

1074 For head-fixed behavior, anticipatory licking was defined to be the number of  
1075 licks within the 1.0 second window prior to water delivery. For freely-moving behavior,  
1076 anticipatory licking was defined as the percentage of time spent licking in the last 1.2  
1077 seconds prior to water delivery. Collection licking was defined as the percentage of time  
1078 spent licking within the 1.0 seconds after water delivery. AUC (area under ROC) was  
1079 calculated for each mouse by comparing the distributions of licks to CS+ trials and to  
1080 CS- trials over a moving window of 20 trials.

1081

1082 Criterion for learning to CS+ odors was defined as the number of trials required  
1083 to display anticipatory licking in over 80% of the CS+ trials. Criterion for learning to CS-  
1084 odors was defined as the number of trials required to display any anticipatory licking in  
1085 less than 20% of the CS- trials. The percentage of trials with anticipatory licking was  
1086 calculated using a moving window with a length that was adjusted to match the  
1087 durations to learn in the different tasks. Window lengths: single-phase head-fixed task =  
1088 20; pre-training in the two-phase head-fixed task = 20; discrimination in the two-phase  
1089 head-fixed task = 10; pre-training in the two-phase freely moving task = 40;  
1090 discrimination in the two-phase discrimination task = 20.

1091

### 1092 ***Image Processing***



1093 Images were first motion-corrected using sub-pixel image registration (Guizar-  
1094 Sicairos et al., 2008). Motion correction was first applied within each trial (75 frames per  
1095 trial), and then across trials by registering the mean intensity image of different trials  
1096 (40-80 trials per imaging session). In some FOVs, we often observed small  
1097 fluorescence changes occurring in large areas ( $> 100 \text{ um} \times 100 \text{ um}$ ) that could be the  
1098 consequence of calcium transients in out-of-focus planes. We eliminated these diffuse  
1099 calcium fluctuations through a spatial low-pass Gaussian filter (length constant, 50  $\text{um}$ ).

1100

### 1101 ***Calcium Transient Analysis***

1102 For ROI identification, we used a MATLAB package for calcium transient analysis  
1103 based on nonnegative matrix factorization (NMF) (Pnevmatikakis et al., 2016). Spatial  
1104 filters that corresponded to neurons were selected, and other signals that did not  
1105 correspond to neural cell bodies (for example, neuropil) were manually deleted. On rare  
1106 occasions, the algorithm classified distinct neurons in close proximity as one neuron,  
1107 and the spatial filter was split manually. On average, 70-100 neurons were extracted,  
1108 and de-noised DF/F was computed for each neuron.

1109

1110 To identify the same neurons across multiple days of imaging sessions, we first  
1111 performed NMF to extract spatial filters corresponding to neurons on each imaging day.  
1112 We then aligned image stacks by performing rigid body registration on the mean  
1113 intensity images (MII) of each imaging day. For example, for a set of imaging data  
1114 acquired across 5 days, we used the MII on day 3 as reference, and transformation  
1115 matrices were derived by aligning MIIs on other days relative to day 3. After alignment,

1116 we pooled all unique and non-overlapping spatial filters from all imaging days into a  
1117 single list. Neuronal cell counts obtained after this step typically exceeded standard  
1118 single-day cell count results by 20-40%. We then back-applied each spatial filter to  
1119 derive optimal cellular outlines corresponding to the same cell on each imaging day. We  
1120 manually assessed whether the back-applied spatial filters on each imaging day  
1121 corresponded to the same cell by evaluating the shapes of the spatial filters while being  
1122 blind to the fluorescence data. This led to the exclusion of 10-20% of all ROIs when  
1123 aligning across 4 or more imaging days.

1124

### 1125 ***Quantification of Significant Neuronal Response***

1126 For each cell, we pooled the DF/F values during the baseline period (the first five  
1127 seconds of each imaging trial prior to odor delivery) of all odor trials to create a  
1128 reference distribution of DF/F values. This was compared to a distribution of pooled  
1129 DF/F values centered on a given frame with a moving window of 3 frames (0.67  
1130 seconds), in which we refer to as the sample distribution. A Mann-Whitney U test was  
1131 performed on the reference and sample distributions to obtain a P-value for each frame.  
1132 Using this method, a P-value was obtained for every frame after odor onset. A cell was  
1133 defined as significantly active on a given imaging day if: 1) the P-value was less than  
1134 0.01 for at least 8 consecutive frames after odor onset and 2) the maximum DF/F during  
1135 the odor delivery period exceeded the DF/F during the baseline period over a set  
1136 threshold. This DF/F threshold was 0.10 for piriform responses, 0.04 for OFC  
1137 responses, and 0.03 for mPFC responses to account for observed differences in

1138 GCaMP6s expression within each area in our transgenic mice. We used this metric to  
1139 quantify the fraction of cells responsive to a stimulus on a given imaging day.

1140

1141       After reversal learning, OFC responses to the old CS+ odors in most neurons did  
1142 not diminish down to amplitudes observed prior to training. We thus quantified the  
1143 fraction of neurons that responded more to CS+ odors than to CS- odors, and vice  
1144 versa, after discrimination learning and after reversal learning. For a neuron to be  
1145 considered to be responding more to CS+ odors than CS- odors, it must have  
1146 statistically significant responses (see above) to both CS+ odors and also respond with  
1147 greater amplitude to CS+ odors than to CS- odors.

1148

#### 1149 ***Response Power***

1150       We defined the response power of a neuronal population to a given odor to be  
1151 the mean excitatory response to that odor. Neuronal responses that were inhibitory  
1152 throughout the entire odor presentation period and the delay period were excluded from  
1153 this analysis because the magnitude of inhibition cannot be reliably measured with  
1154 genetically encoded calcium indicators, especially given low baseline firing rates.

1155

#### 1156 ***Correlation Analysis***

1157       The maximum trial-averaged DF/F response between odor onset and water  
1158 onset for all neurons was computed, forming a vector that corresponds to the population  
1159 activity evoked by a given odor. The Pearson product-moment correlation coefficient  
1160 was then calculated based on two such population activity vectors. This was used to

1161 compute the correlation of population activities evoked by the same odor across  
1162 different training days as well as the correlation of population activities evoked by  
1163 different odors within a training day.

1164 To correlate an odor ensemble with itself (for example, the diagonal entries of  
1165 Figure 1H), trials of a given odor were split into two equal halves after random shuffling,  
1166 and the correlation was then calculated using the trial-averaged DF/F responses of the  
1167 split data. This was repeated 100 times.

1168

### 1169 ***Decoding***

1170 Support vector machines with linear kernels were constructed using the scikit-  
1171 learn library in Python. For each odor trial, we created a vector that corresponds to the  
1172 population activity, based on the maximum DF/F between odor onset and water onset  
1173 for each trial. The number of neurons used was standardized across all animals in all  
1174 conditions to be 40 and they were randomly chosen. For the decoding of odors across  
1175 days, we trained the decoder using odor trials from a given day and tested decoding  
1176 performance with odor trials on all other days. For decoding trials within the same day,  
1177 we trained decoders using 5-fold cross-validation. Decoding simulations were repeated  
1178 100 times per condition, drawing a new and random set of 40 neurons for each  
1179 condition.

1180

1181 For decoding odor value, CS+1 and CS+2 odor trials were pooled together, and CS-1  
1182 and CS-2 were pooled together, and each group had a different label. For decoding  
1183 CS+ odor identity, only CS+1 trials and CS+2 trials were used, and each group had a

1184 different label. For decoding CS- odor identity, only CS-1 trials and CS-2 trials were  
1185 used, and each group had a different label. For decoding odor identity, CS+1, CS+2,  
1186 CS-1, and CS-2 trials were used and have different labels. The strategy used for multi-  
1187 class decoding of odor identities is the “one-against-one” multi-class classification  
1188 approach. The values for chance performance for these conditions using random  
1189 shuffling with 50 repetitions were: odor valence 50%, CS+ identity 50%, CS- identity  
1190 50%, odor identity 25%.

1337

- 1338 Allen, W.E., Chen, M.Z., Pichamoorthy, N., Tien, R.H., Pachitariu, M., Luo, L., and  
1339 Deisseroth, K. (2019). Thirst regulates motivated behavior through modulation of  
1340 brainwide neural population dynamics. *Science* (80- ).
- 1341 Barretto, R.P., Messerschmidt, B., and Schnitzer, M.J. (2009). In vivo fluorescence  
1342 imaging with high-resolution microlenses. *Nat Methods* 6, 511–512.
- 1343 Benna, M.K., and Fusi, S. (2016). Computational principles of synaptic memory  
1344 consolidation. *Nat. Neurosci.*
- 1345 Birrell, J.M., and Brown, V.J. (2000). Medial Frontal Cortex Mediates Perceptual  
1346 Attentional Set Shifting in the Rat. *J. Neurosci.*
- 1347 Bissonette, G.B., Martins, G.J., Franz, T.M., Harper, E.S., Schoenbaum, G., and Powell,  
1348 E.M. (2008). Double Dissociation of the Effects of Medial and Orbital Prefrontal Cortical  
1349 Lesions on Attentional and Affective Shifts in Mice. *J. Neurosci.*
- 1350 Bontempi, B., Laurent-Demir, C., Destrade, C., and Jaffard, R. (1999). Time-dependent  
1351 reorganization of brain circuitry underlying long-term memory storage. *Nature* 400, 671–  
1352 675.
- 1353 Bouton, M.E. (2004). Context and behavioral processes in extinction. *Learn. Mem.*
- 1354 Bozza, T., McGann, J.P., Mombaerts, P., and Wachowiak, M. (2004). In vivo imaging of  
1355 neuronal activity by targeted expression of a genetically encoded probe in the mouse.  
1356 *Neuron* 42, 9–21.
- 1357 Buck, L., and Axel, R. (1991). A novel multigene family may encode odorant receptors:  
1358 a molecular basis for odor recognition. *Cell* 65, 175–187.
- 1359 Buonomano, D. V, and Merzenich, M.M. (1998). Cortical plasticity: from synapses to  
1360 maps. *Annu. Rev. Neurosci.* 21, 149–186.
- 1361 Burke, K.A., Franz, T.M., Miller, D.N., and Schoenbaum, G. (2008). The role of the  
1362 orbitofrontal cortex in the pursuit of happiness and more specific rewards. *Nature.*
- 1363 Chen, C.F., Zou, D.J., Altomare, C.G., Xu, L., Greer, C.A., and Firestein, S.J. (2014).  
1364 Nonsensory target-dependent organization of piriform cortex. *Proc Natl Acad Sci U S A*  
1365 111, 16931–16936.
- 1366 Chen, T.W., Wardill, T.J., Sun, Y., Pulver, S.R., Renninger, S.L., Baohan, A., Schreiter,  
1367 E.R., Kerr, R.A., Orger, M.B., Jayaraman, V., et al. (2013). Ultrasensitive fluorescent  
1368 proteins for imaging neuronal activity. *Nature* 499, 295–300.
- 1369 Choi, G.B., Stettler, D.D., Kallman, B.R., Bhaskar, S.T., Fleischmann, A., and Axel, R.  
1370 (2011). Driving opposing behaviors with ensembles of piriform neurons. *Cell* 146, 1004–  
1371 1015.
- 1372 Chudasama, Y., and Robbins, T.W. (2003). Dissociable contributions of the orbitofrontal  
1373 and infralimbic cortex to pavlovian autoshaping and discrimination reversal learning:  
1374 further evidence for the functional heterogeneity of the rodent frontal cortex. *J. Neurosci.*  
1375 23, 8771–8780.

- 1376 Chuong, A.S., Miri, M.L., Buskamp, V., Matthews, G.A.C., Acker, L.C., Sørensen, A.T.,  
1377 Young, A., Klapoetke, N.C., Henninger, M.A., Kodandaramaiah, S.B., et al. (2014).  
1378 Noninvasive optical inhibition with a red-shifted microbial rhodopsin. *Nat. Neurosci.* *17*,  
1379 1123–1129.
- 1380 Critchley, H.D., and Rolls, E.T. (1996). Hunger and satiety modify the responses of  
1381 olfactory and visual neurons in the primate orbitofrontal cortex. *J Neurophysiol* *75*,  
1382 1673–1686.
- 1383 Davison, I.G., and Ehlers, M.D. (2011). Neural circuit mechanisms for pattern detection  
1384 and feature combination in olfactory cortex. *Neuron* *70*, 82–94.
- 1385 Denk, W., Strickler, J.H., and Webb, W.W. (1990). Two-photon laser scanning  
1386 fluorescence microscopy. *Science* (80- ).
- 1387 Diodato, A., Ruinat De Brimont, M., Yim, Y.S., Derian, N., Perrin, S., Pouch, J.,  
1388 Klatzmann, D., Garel, S., Choi, G.B., and Fleischmann, A. (2016). Molecular signatures  
1389 of neural connectivity in the olfactory cortex. *Nat. Commun.*
- 1390 Feierstein, C.E., Quirk, M.C., Uchida, N., Sosulski, D.L., and Mainen, Z.F. (2006).  
1391 Representation of spatial goals in rat orbitofrontal cortex. *Neuron* *51*, 495–507.
- 1392 Feldman, D.E. (2009). Synaptic Mechanisms for Plasticity in Neocortex. *Annu. Rev.*  
1393 *Neurosci.*
- 1394 Ferenczi, E.A., Zalocusky, K.A., Liston, C., Grosenick, L., Warden, M.R., Amatya, D.,  
1395 Katovich, K., Mehta, H., Patenaude, B., Ramakrishnan, C., et al. (2016). Prefrontal  
1396 cortical regulation of brainwide circuit dynamics and reward-related behavior. *Science*  
1397 (80- ).
- 1398 Fusi, S., Drew, P.J., and Abbott, L.F. (2005). Cascade models of synaptically stored  
1399 memories. *Neuron*.
- 1400 Gallagher, M., McMahan, R.W., and Schoenbaum, G. (1999). Orbitofrontal cortex and  
1401 representation of incentive value in associative learning. *J Neurosci* *19*, 6610–6614.
- 1402 Ghosh, S., Larson, S.D., Hefzi, H., Marnoy, Z., Cutforth, T., Dokka, K., and Baldwin,  
1403 K.K. (2011). Sensory maps in the olfactory cortex defined by long-range viral tracing of  
1404 single neurons. *Nature* *472*, 217–220.
- 1405 Godfrey, P.A., Malnic, B., and Buck, L.B. (2004). The mouse olfactory receptor gene  
1406 family. *Proc. Natl. Acad. Sci.* *101*, 2156–2161.
- 1407 Goshen, I., Brodsky, M., Prakash, R., Wallace, J., Gradinaru, V., Ramakrishnan, C., and  
1408 Deisseroth, K. (2011). Dynamics of Retrieval Strategies for Remote Memories. *Cell* *147*,  
1409 678–689.
- 1410 Gottfried, J.A., O’Doherty, J., and Dolan, R.J. (2003). Encoding predictive reward value  
1411 in human amygdala and orbitofrontal cortex. *Science* *301*, 1104–1107.
- 1412 Gradinaru, V., Thompson, K.R., and Deisseroth, K. (2008). eNpHR: a *Natronomonas*  
1413 halorhodopsin enhanced for optogenetic applications. *Brain Cell Biol* *36*, 129–139.
- 1414 Guizar-Sicairos, M., Thurman, S.T., and Fienup, J.R. (2008). Efficient subpixel image  
1415 registration algorithms. *Opt. Lett.*

- 1416 Illig, K.R., and Haberly, L.B. (2003). Odor-evoked activity is spatially distributed in  
1417 piriform cortex. *J. Comp. Neurol.*
- 1418 Iurilli, G., and Datta, S.R. (2017). Population Coding in an Innately Relevant Olfactory  
1419 Area. *Neuron.*
- 1420 Izquierdo, A., Suda, R.K., and Murray, E.A. (2004). Bilateral orbital prefrontal cortex  
1421 lesions in rhesus monkeys disrupt choices guided by both reward value and reward  
1422 contingency. *J. Neurosci.* *24*, 7540–7548.
- 1423 Johnson, D.M., Illig, K.R., Behan, M., and Haberly, L.B. (2000). New features of  
1424 connectivity in piriform cortex visualized by intracellular injection of pyramidal cells  
1425 suggest that “primary” olfactory cortex functions like “association” cortex in other  
1426 sensory systems. *J. Neurosci.* *20*, 6974–6982.
- 1427 Jung, J.C., Mehta, A.D., Aksay, E., Stepnoski, R., and Schnitzer, M.J. (2004). In Vivo  
1428 Mammalian Brain Imaging Using One- and Two-Photon Fluorescence Microendoscopy.  
1429 *J. Neurophysiol.*
- 1430 Kepecs, A., Uchida, N., Zariwala, H.A., and Mainen, Z.F. (2008). Neural correlates,  
1431 computation and behavioural impact of decision confidence. *Nature* *455*, 227–231.
- 1432 Kim, J.J., and Fanselow, M.S. (1992). Modality-specific retrograde amnesia of fear.  
1433 *Science* (80- ).
- 1434 Kim, C.K., Ye, L., Jennings, J.H., Pichamoorthy, N., Tang, D.D., Yoo, A.C.W.,  
1435 Ramakrishnan, C., and Deisseroth, K. (2017). Molecular and Circuit-Dynamical  
1436 Identification of Top-Down Neural Mechanisms for Restraint of Reward Seeking. *Cell.*
- 1437 Kitamura, T., Ogawa, S.K., Roy, D.S., Okuyama, T., Morrissey, M.D., Smith, L.M.,  
1438 Redondo, R.L., and Tonegawa, S. (2017). Engrams and circuits crucial for systems  
1439 consolidation of a memory. *Science* *356*, 73–78.
- 1440 Lipton, P.A., Alvarez, P., and Eichenbaum, H. (1999). Crossmodal associative memory  
1441 representations in rodent orbitofrontal cortex. *Neuron* *22*, 349–359.
- 1442 Madisen, L., Garner, A.R., Shimaoka, D., Chuong, A.S., Klapoetke, N.C., Li, L., van der  
1443 Bourg, A., Niino, Y., Egolf, L., Monetti, C., et al. (2015). Transgenic mice for  
1444 intersectional targeting of neural sensors and effectors with high specificity and  
1445 performance. *Neuron* *85*, 942–958.
- 1446 McClelland, J.L., McNaughton, B.L., and O’Reilly, R.C. (1995). Why there are  
1447 complementary learning systems in the hippocampus and neocortex: Insights from the  
1448 successes and failures of connectionist models of learning and memory. *Psychol. Rev.*
- 1449 Miyamichi, K., Amat, F., Moussavi, F., Wang, C., Wickersham, I., Wall, N.R., Taniguchi,  
1450 H., Tasic, B., Huang, Z.J., He, Z., et al. (2011). Cortical representations of olfactory  
1451 input by trans-synaptic tracing. *Nature* *472*, 191–196.
- 1452 Mombaerts, P., Wang, F., Dulac, C., Chao, S.K., Nemes, A., Mendelsohn, M.,  
1453 Edmondson, J., and Axel, R. (1996). Visualizing an Olfactory Sensory Map. *Cell* *87*,  
1454 675–686.
- 1455 Namboodiri, V.M.K., Otis, J.M., van Heeswijk, K., Voets, E.S., Alghorazi, R.A.,



- 1456 Rodriguez-Romaguera, J., Mihalas, S., and Stuber, G.D. (2019). Single-cell activity  
1457 tracking reveals that orbitofrontal neurons acquire and maintain a long-term memory to  
1458 guide behavioral adaptation. *Nat. Neurosci.*
- 1459 Ostlund, S.B., and Balleine, B.W. (2005). Lesions of medial prefrontal cortex disrupt the  
1460 acquisition but not the expression of goal-directed learning. *J. Neurosci.* *25*, 7763–7770.
- 1461 Ostlund, S.B., and Balleine, B.W. (2007). Orbitofrontal Cortex Mediates Outcome  
1462 Encoding in Pavlovian But Not Instrumental Conditioning. *J. Neurosci.*
- 1463 Otis, J.M., Namboodiri, V.M.K., Matan, A.M., Voets, E.S., Mohorn, E.P., Kosyk, O.,  
1464 McHenry, J.A., Robinson, J.E., Resendez, S.L., Rossi, M.A., et al. (2017). Prefrontal  
1465 cortex output circuits guide reward seeking through divergent cue encoding. *Nature*  
1466 *543*, 103–107.
- 1467 Pachitariu, M., Steinmetz, N.A., Kadir, S.N., Carandini, M., and Harris, K.D. (2016). Fast  
1468 and accurate spike sorting of high-channel count probes with KiloSort. In *Advances in*  
1469 *Neural Information Processing Systems 29*, D.D. Lee, M. Sugiyama, U. V Luxburg, I.  
1470 Guyon, and R. Garnett, eds. (Curran Associates, Inc.), pp. 4448–4456.
- 1471 Padoa-Schioppa, C., and Assad, J.A. (2006). Neurons in the orbitofrontal cortex encode  
1472 economic value. *Nature* *441*, 223–226.
- 1473 Pnevmatikakis, E.A., Soudry, D., Gao, Y., Machado, T.A., Merel, J., Pfau, D., Reardon,  
1474 T., Mu, Y., Lacefield, C., Yang, W., et al. (2016). Simultaneous Denoising,  
1475 Deconvolution, and Demixing of Calcium Imaging Data. *Neuron* *89*, 285–299.
- 1476 Poo, C., and Isaacson, J.S. (2009). Odor representations in olfactory cortex: “sparse”  
1477 coding, global inhibition, and oscillations. *Neuron* *62*, 850–861.
- 1478 Price, J.L. (1985). Beyond the primary olfactory cortex: Olfactory-related areas in the  
1479 neocortex, thalamus and hypothalamus. *Chem. Senses.*
- 1480 Price, J.L., and Powell, T.P. (1970). The mitral and short axon cells of the olfactory bulb.  
1481 *J Cell Sci* *7*, 631–651.
- 1482 Ramus, S.J., and Eichenbaum, H. (2000). Neural correlates of olfactory recognition  
1483 memory in the rat orbitofrontal cortex. *J Neurosci* *20*, 8199–8208.
- 1484 Rennaker, R.L., Chen, C.F., Ruyle, A.M., Sloan, A.M., and Wilson, D.A. (2007). Spatial  
1485 and temporal distribution of odorant-evoked activity in the piriform cortex. *J Neurosci* *27*,  
1486 1534–1542.
- 1487 Ressler, K.J., Sullivan, S.L., and Buck, L.B. (1993). A zonal organization of odorant  
1488 receptor gene expression in the olfactory epithelium. *Cell* *73*, 597–609.
- 1489 Ressler, K.J., Sullivan, S.L., and Buck, L.B. (1994). Information coding in the olfactory  
1490 system: evidence for a stereotyped and highly organized epitope map in the olfactory  
1491 bulb. *Cell* *79*, 1245–1255.
- 1492 Roesch, M.R., Stalnaker, T.A., and Schoenbaum, G. (2007). Associative encoding in  
1493 anterior piriform cortex versus orbitofrontal cortex during odor discrimination and  
1494 reversal learning. *Cereb. Cortex* *17*, 643–652.
- 1495 Rossant, C., Kadir, S.N., Goodman, D.F.M., Schulman, J., Hunter, M.L.D., Saleem,

- 1496 A.B., Grosmark, A., Belluscio, M., Denfield, G.H., Ecker, A.S., et al. (2016). Spike  
1497 sorting for large, dense electrode arrays. *Nat. Neurosci.*
- 1498 Roxin, A., and Fusi, S. (2013). Efficient Partitioning of Memory Systems and Its  
1499 Importance for Memory Consolidation. *PLoS Comput. Biol.*
- 1500 Royer, S., Zemelman, B. V., Barbic, M., Losonczy, A., Buzsáki, G., and Magee, J.C.  
1501 (2010). Multi-array silicon probes with integrated optical fibers: Light-assisted  
1502 perturbation and recording of local neural circuits in the behaving animal. *Eur. J.*  
1503 *Neurosci.*
- 1504 Schoenbaum, G., and Eichenbaum, H. (1995). Information Coding in the Rodent  
1505 Prefrontal Cortex .1. Single-Neuron Activity in Orbitofrontal Cortex Compared with That  
1506 in Piriform Cortex. *J. Neurophysiol.* *74*, 733–750.
- 1507 Schoenbaum, G., Chiba, A.A., and Gallagher, M. (1998). Orbitofrontal cortex and  
1508 basolateral amygdala encode expected outcomes during learning. *Nat. Neurosci.* *1*,  
1509 155–159.
- 1510 Schoenbaum, G., Chiba, A.A., and Gallagher, M. (1999). Neural encoding in  
1511 orbitofrontal cortex and basolateral amygdala during olfactory discrimination learning. *J.*  
1512 *Neurosci.* *19*, 1876–1884.
- 1513 Schoenbaum, G., Nugent, S.L., Saddoris, M.P., and Setlow, B. (2002). Orbitofrontal  
1514 lesions in rats impair reversal but not acquisition of go, no-go odor discriminations.  
1515 *Neuroreport* *13*, 885–890.
- 1516 Schoenbaum, G., Setlow, B., Nugent, S.L., Saddoris, M.P., and Gallagher, M. (2003).  
1517 Lesions of orbitofrontal cortex and basolateral amygdala complex disrupt acquisition of  
1518 odor-guided discriminations and reversals. *Learn Mem* *10*, 129–140.
- 1519 Schultz, W. (2016). Dopamine reward prediction error coding. *Dialogues Clin. Neurosci.*
- 1520 Schwabe, K., Ebert, U., and Loscher, W. (2004). The central piriform cortex: anatomical  
1521 connections and anticonvulsant effect of GABA elevation in the kindling model.  
1522 *Neuroscience* *126*, 727–741.
- 1523 Sosulski, D.L., Bloom, M.L., Cutforth, T., Axel, R., and Datta, S.R. (2011). Distinct  
1524 representations of olfactory information in different cortical centres. *Nature* *472*, 213–  
1525 216.
- 1526 Squire, L.R., and Alvarez, P. (1995). Retrograde amnesia and memory consolidation: a  
1527 neurobiological perspective. *Curr. Opin. Neurobiol.*
- 1528 Stalnaker, T.A., Franz, T.M., Singh, T., and Schoenbaum, G. (2007). Basolateral  
1529 Amygdala Lesions Abolish Orbitofrontal-Dependent Reversal Impairments. *Neuron.*
- 1530 Stettler, D.D., and Axel, R. (2009). Representations of Odor in the Piriform Cortex.  
1531 *Neuron* *63*, 854–864.
- 1532 Sugai, T., Miyazawa, T., Fukuda, M., Yoshimura, H., and Onoda, N. (2005). Odor-  
1533 concentration coding in the guinea-pig piriform cortex. *Neuroscience.*
- 1534 Takehara-Nishiuchi, K., and McNaughton, B.L. (2008). Spontaneous changes of  
1535 neocortical code for associative memory during consolidation. *Science* (80- ).

- 1536 Thorpe, S.J., Rolls, E.T., and Maddison, S. (1983). The orbitofrontal cortex: neuronal  
1537 activity in the behaving monkey. *Exp Brain Res* 49, 93–115.
- 1538 Tremblay, L., and Schultz, W. (1999). Relative reward preference in primate  
1539 orbitofrontal cortex. *Nature* 398, 704–708.
- 1540 Vassar, R., Chao, S.K., Sitcheran, R., Nuñez, J.M., Vosshall, L.B., and Axel, R. (1994).  
1541 Topographic organization of sensory projections to the olfactory bulb. *Cell* 79, 981–991.
- 1542 Vong, L., Ye, C., Yang, Z., Choi, B., Chua Jr., S., and Lowell, B.B. (2011). Leptin action  
1543 on GABAergic neurons prevents obesity and reduces inhibitory tone to POMC neurons.  
1544 *Neuron* 71, 142–154.
- 1545 Zhan, C., and Luo, M. (2010). Diverse patterns of odor representation by neurons in the  
1546 anterior piriform cortex of awake mice. *J Neurosci* 30, 16662–16672.
- 1547 Zhang, X., and Firestein, S. (2002). The olfactory receptor gene superfamily of the  
1548 mouse. *Nat Neurosci* 5, 124–133.
- 1549